Bootstrapping the Coronal Magnetic Field with STEREO

Markus Aschwanden
Anne Sandman and David Alexander

Lockheed Martin ATC - Solar & Astrophysics Laboratory
Rice University, Houston, TX

STEREO Science Working Group 21, 22-26 March 2010

http://www.lmsal.com/~aschwand/ppt/2010_STEREO_Dublin.ppt

Outline of Talk :

1) Problem: Discrepancy between magnetogram-based magnetic field extrapolations and stereoscopically triangulated 3D loops

2) "The usual suspects"

3) Stereoscopic Triangulation of Coronal Loops

4) Bootstrapping method: Theory

5) Bootstrapping method: Forward-Fitting to Observations

6) Conclusions and Outlook

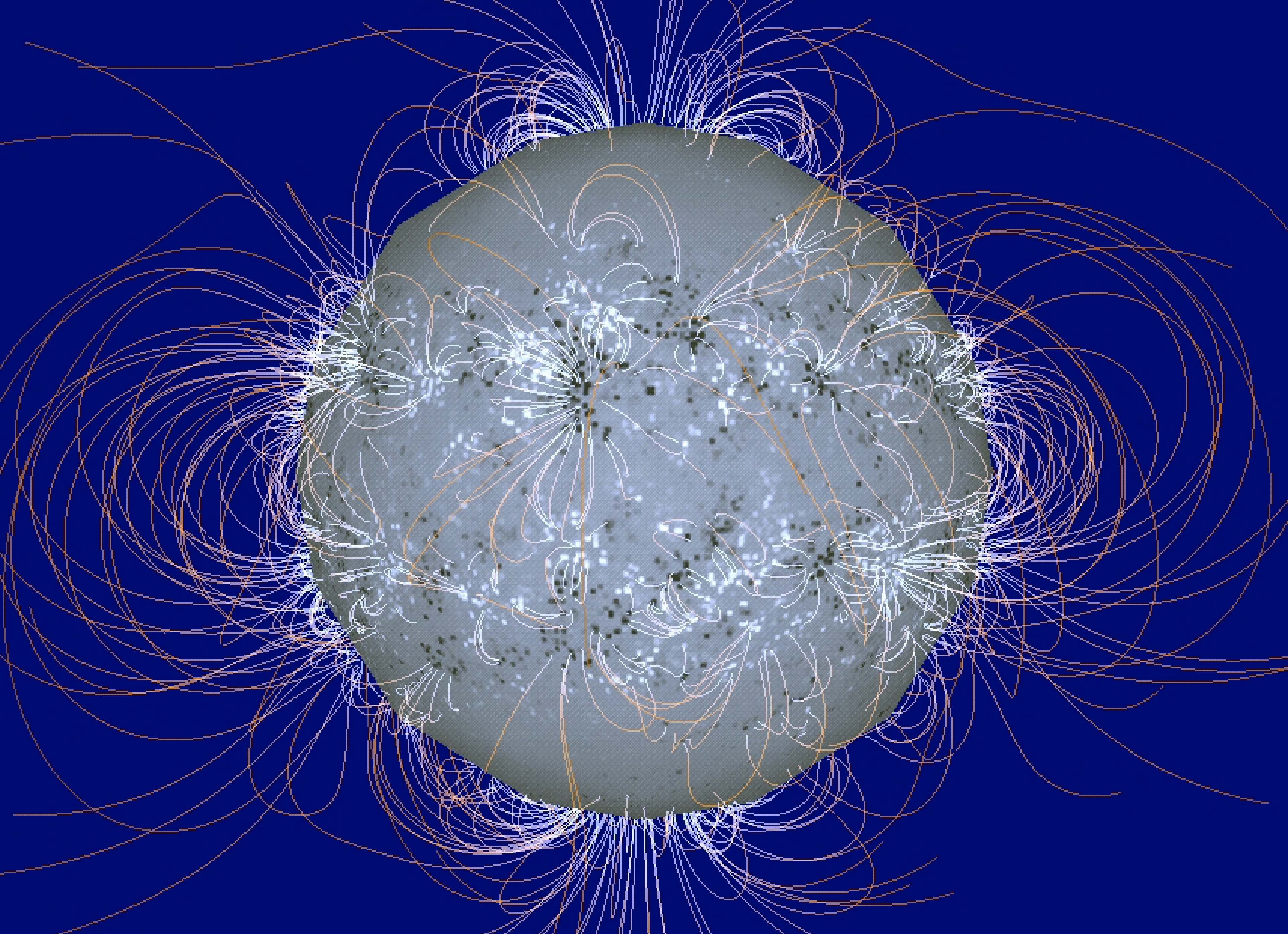

Potential Field Source Surface (PFSS) model: Extrapolation of full-Sun magnetogram

Potential field and constant-alpha extrapolations

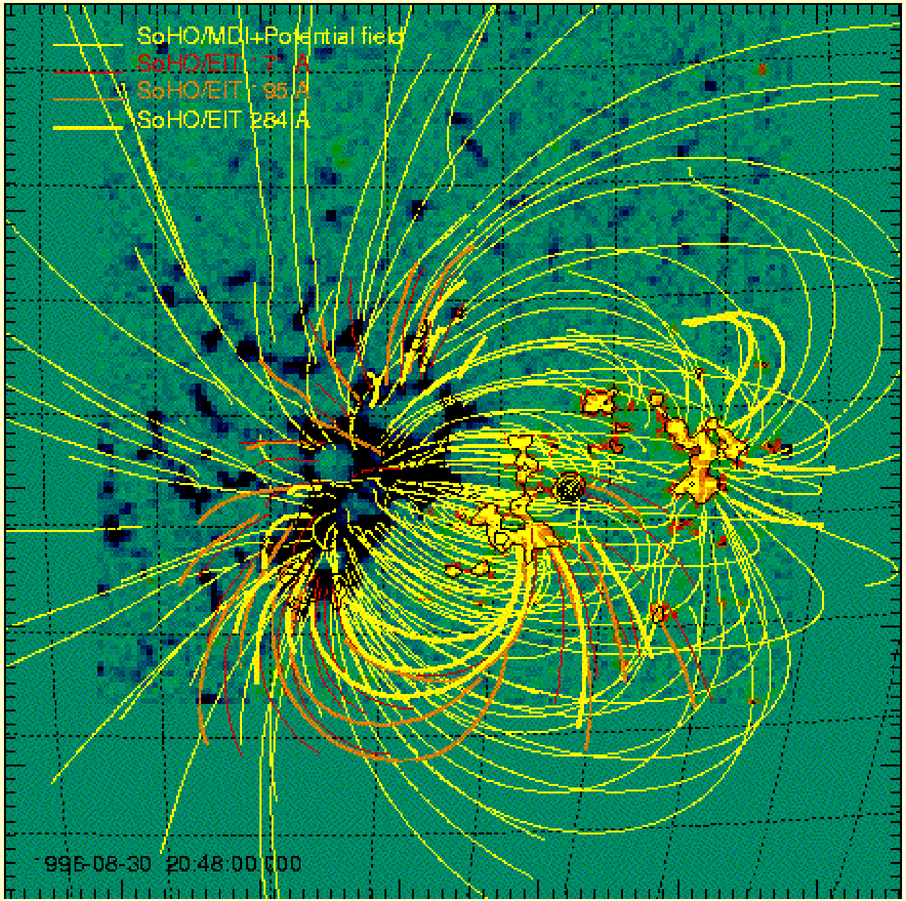

Aschwanden et al. 1999

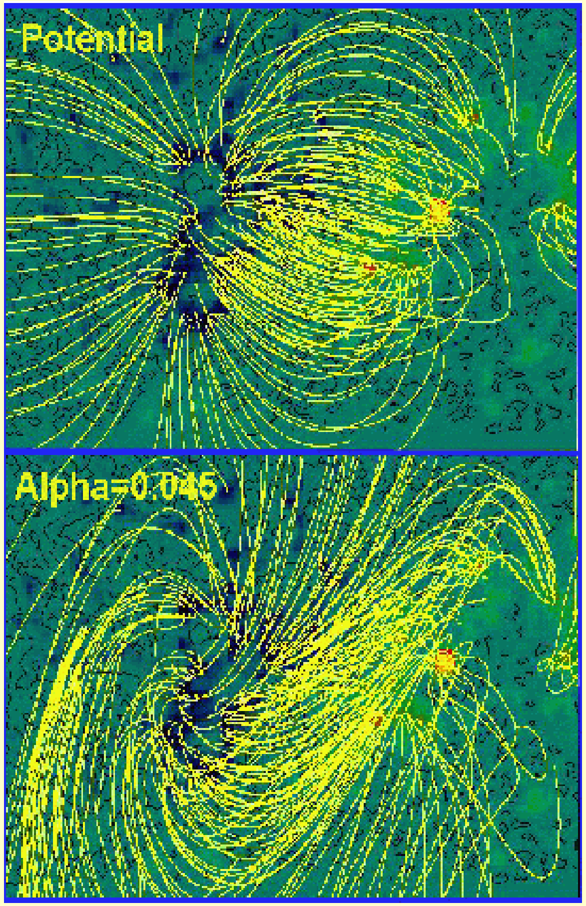

Alan Gary

Stereoscopically reconstructed 3D geometries can constrain theoretical magnetic field models. A computed potential field B(x,y,z) based on SoHO/MDI magnetograms does not match EIT-traced loops observed in EUV (171, 195, 284 A), while a non-potential (linear) force-free model with a=0.045 matches better.

Comparison of PTA Models & Observation

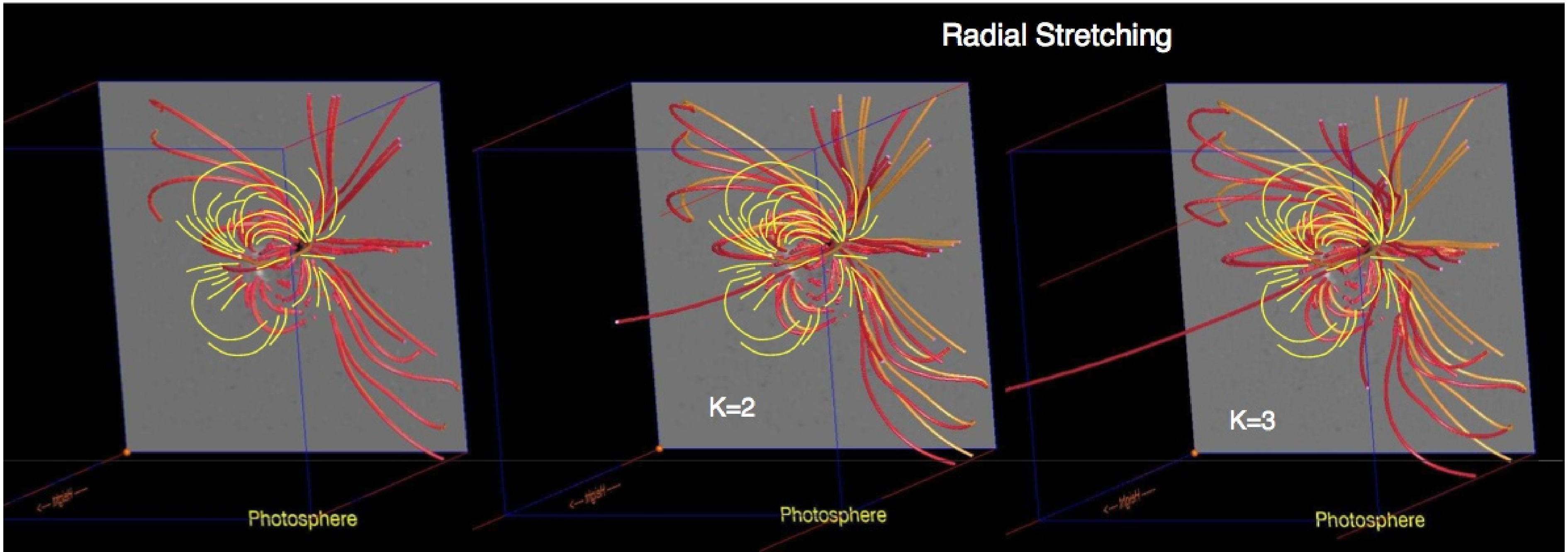

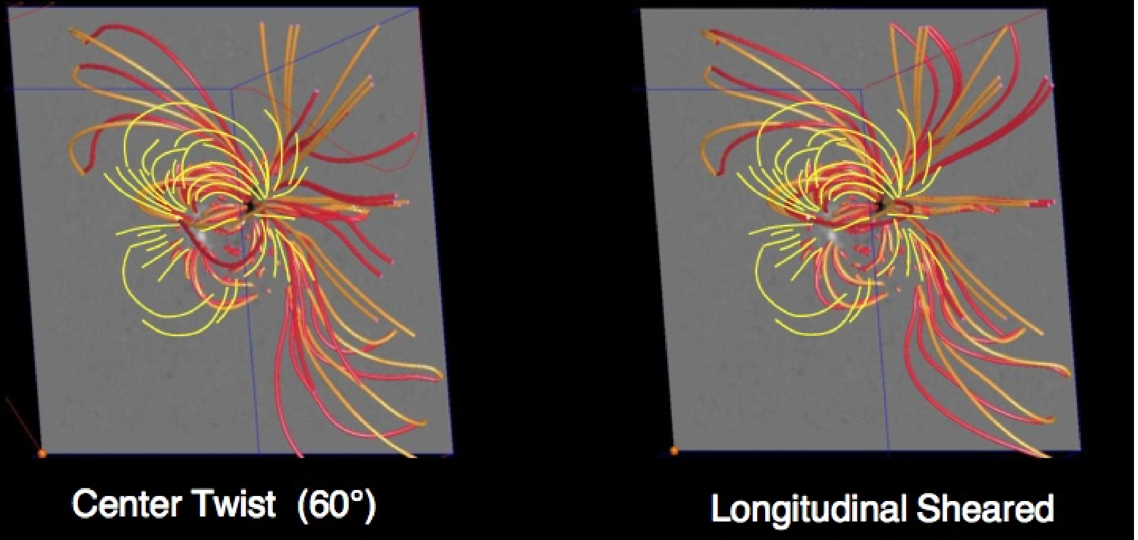

Development items to be included

1) Identify EIS/XRT loops
2) Employ vector magnetograms and NLFFF models
3) Complete L_F minimization process
4) Use STEREO results in a 3D implementation

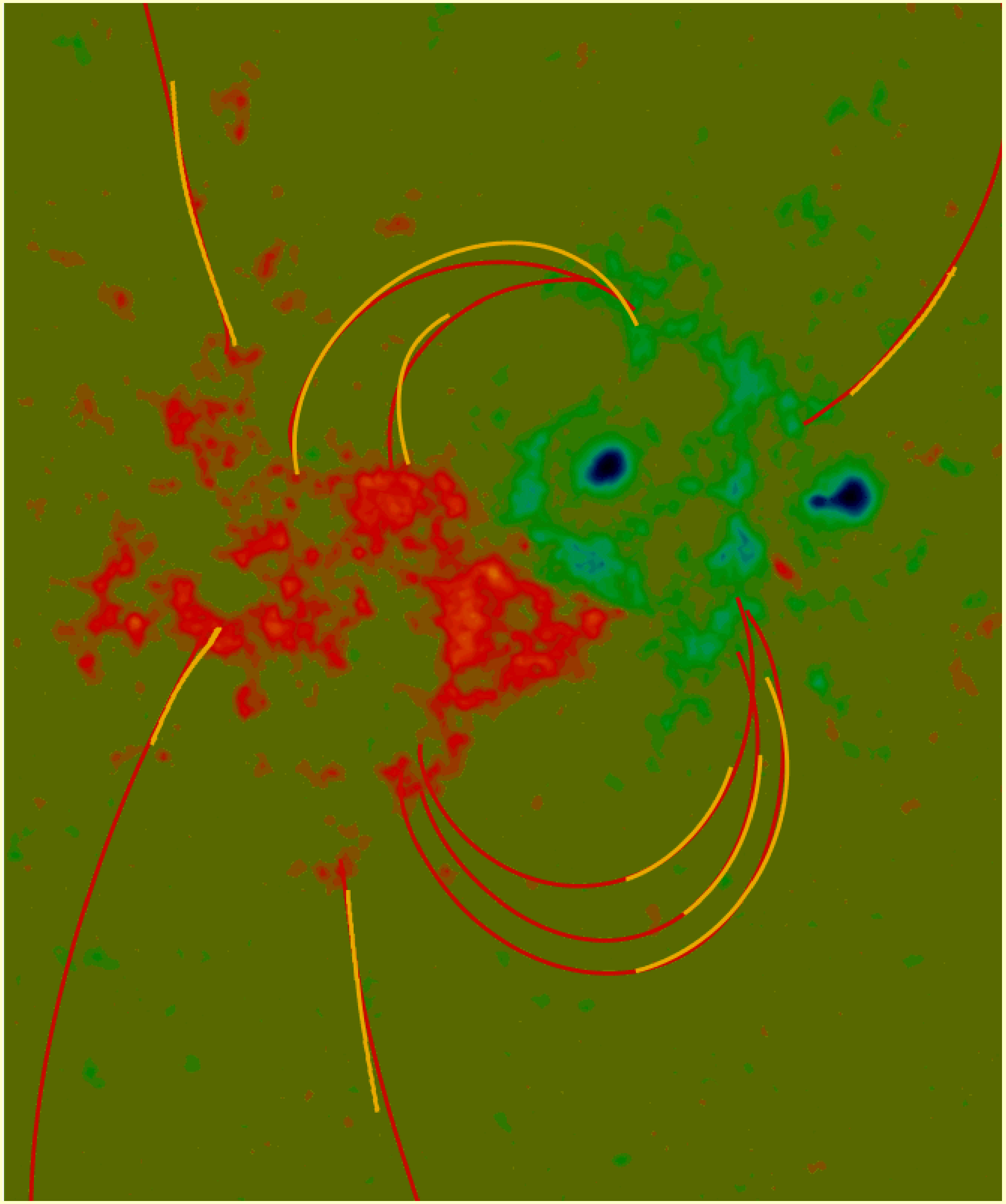

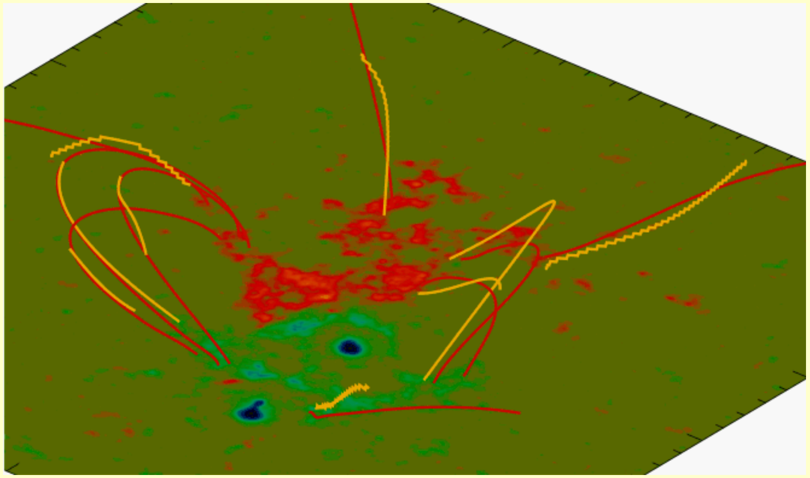

Active region loops reconstructed
from STEREO/EUVI A+B (yellow)
and calculated from
MDI magnetograms and a
force-free magnetic field model
show significant differences,
in particular for open field lines.

Feng et al. (2007, ApJ 671, L205)

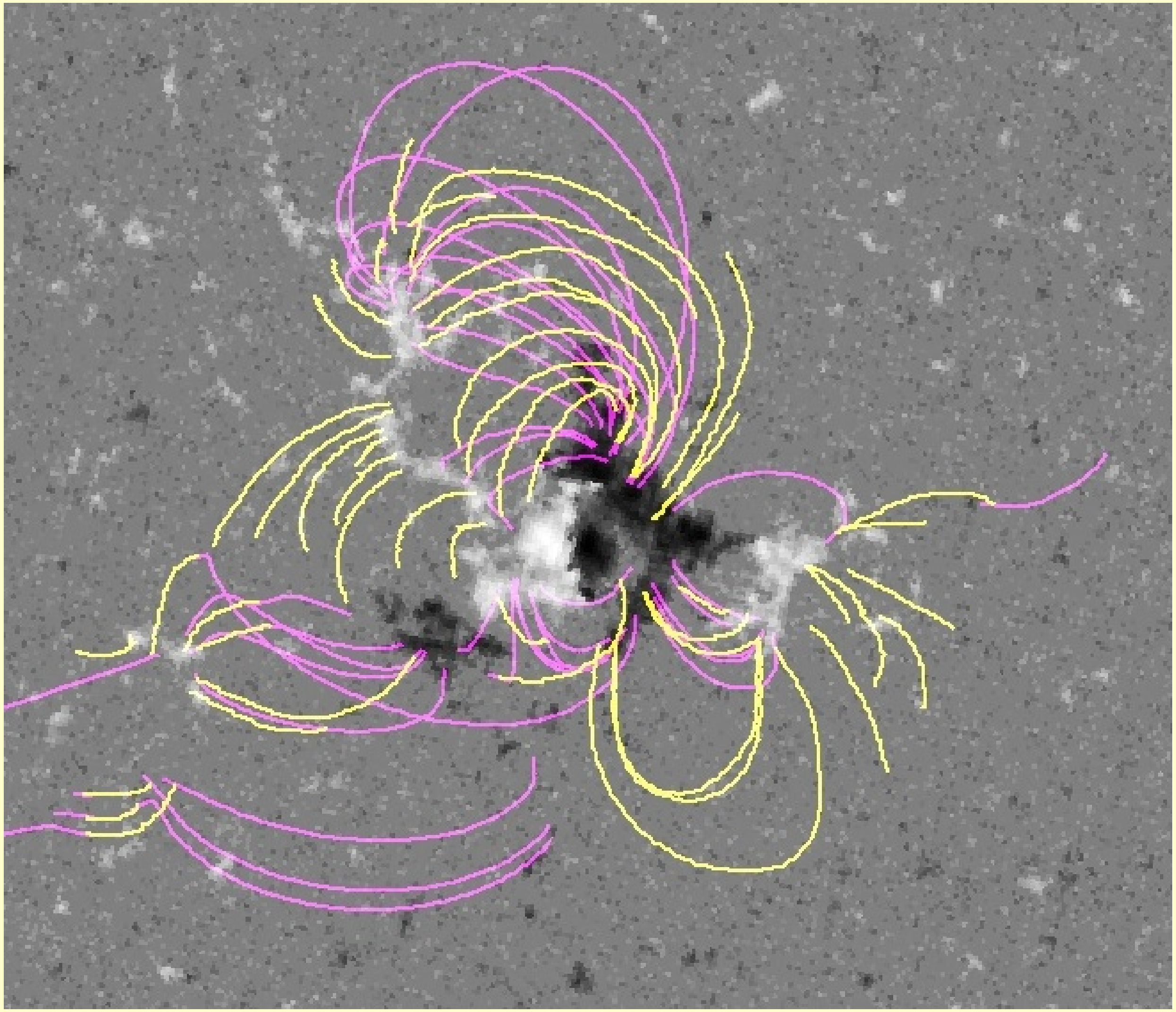

(courtesy of J.P.Wuelser)

Comparison of EUVI loops traced stereoscopically with “potential field source surface” (PFSS) model extrapolated from SoHO/MDI magnetogram:

--> Note significantly different connectivities !

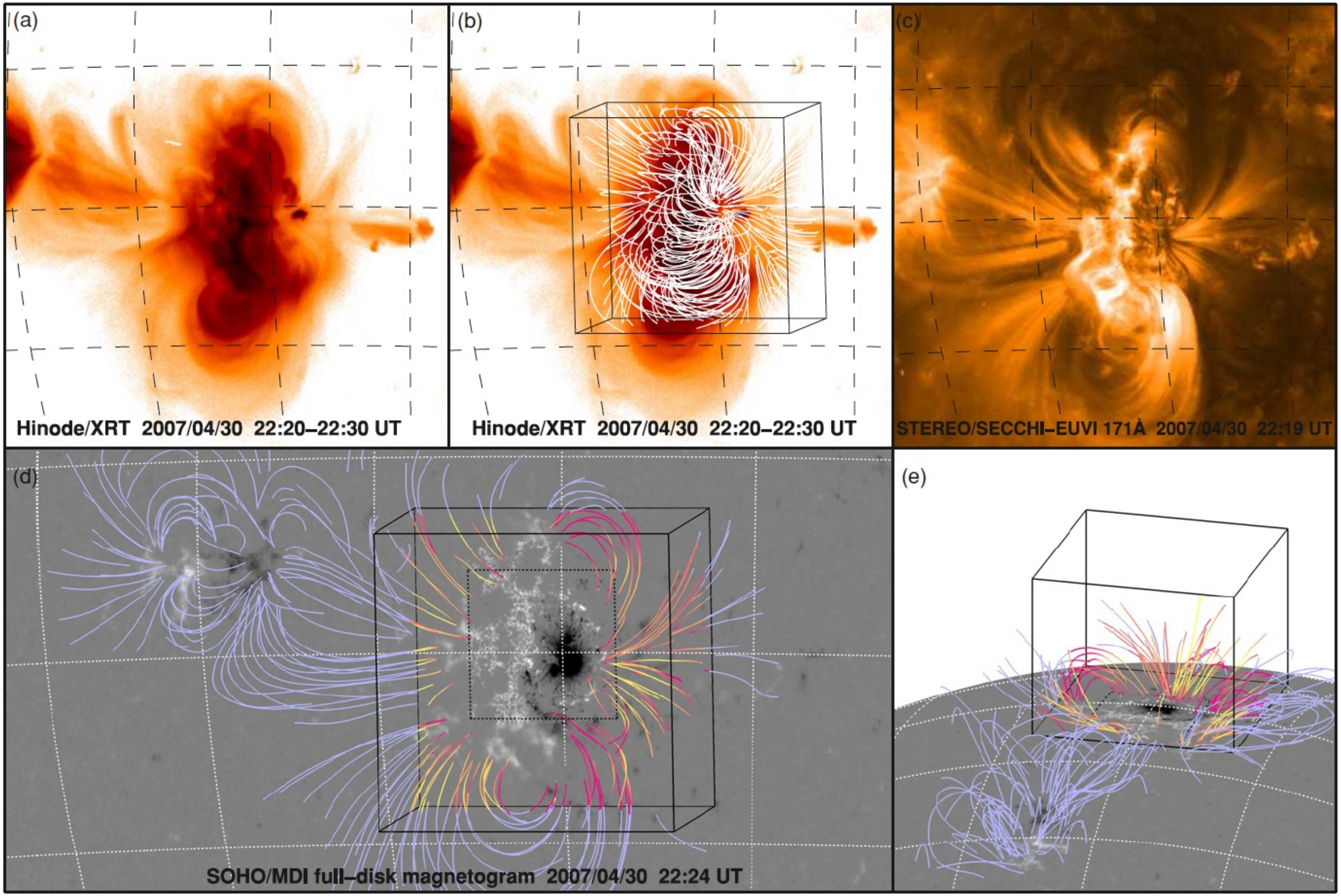

Figure 1. Series of co-aligned images of AR 10953 (with the same 10° gridlines drawn on all images for reference). (*a*) Time-averaged and logarithmically scaled *Hinode*/XRT soft X-ray image, and (*b*) with the best-fit Wh^- model field lines overlaid. (*c*) *STEREO-A*/SECCHI–EUVI 171 Å image. (*d*) Trajectories of loops, as viewed from the perspective of an observer located along the Sun–Earth line of sight and determined stereoscopically from contemporaneous pairs of images from the two *STEREO* spacecraft. (*e*) Same visualization as panel (*d*) but viewed from the side. The solid black cubes in panels (*d*) and (*e*) outline the full 320 × 320 × 256 pixel NLFFF computational domain, and the interior dotted black square outlines the base of the smaller 160 × 160 × 160 pixel volume (covering most of the *Hinode*/SOT–SP scan area) used for the field line maps of Figure 2 and for the metrics in Table 1. The *STEREO*-loop points are colored blue if outside the NLFFF computational domain, or are colored according to their misalignment angle ϕ made with the field lines from the Wh^- solution. Yellow is indicative of $\phi < 5°$, red of $\phi > 45°$, with a continuous progression from yellow through orange to red for $5° < \phi < 45°$. On the bottom face of the large cube is displayed the B_z map used during the NLFFF modeling, which includes higher resolution data from *Hinode*/SOT–SP embedded in *SOHO*/MDI full-disk magnetogram data. The magnetogram images saturate at ±1500 Mx cm^{-2}.

DeRosa et al. (2009)

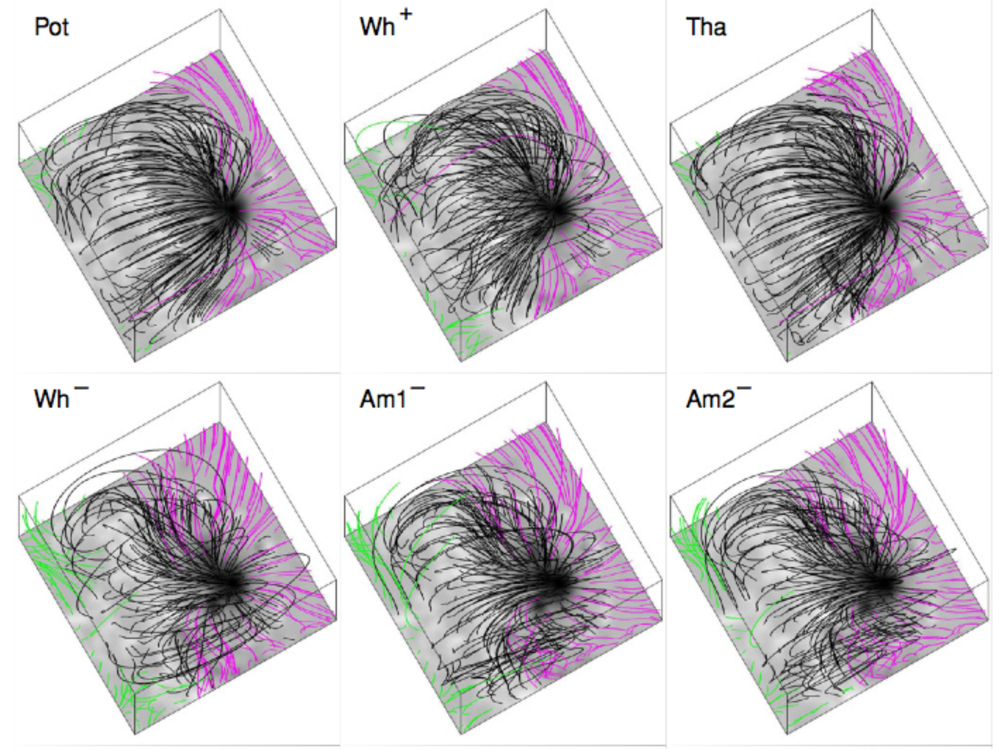

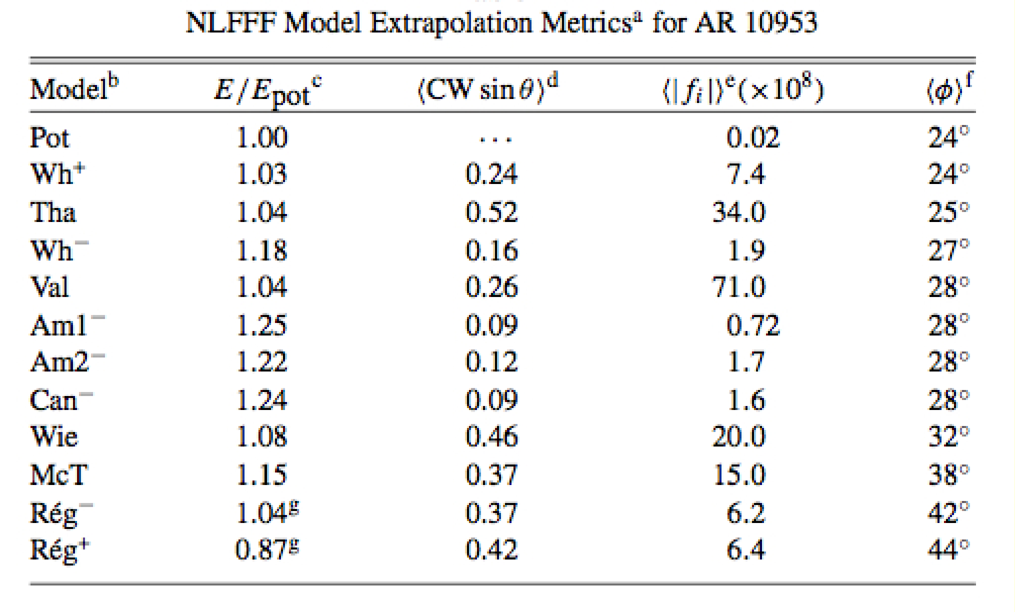

NLFFF Model Extrapolation Metrics[a] for AR 10953

Model[b]	$E/E_{\rm pot}$[c]	$\langle {\rm CW} \sin\theta \rangle$[d]	$\langle \lvert f_i \rvert \rangle$[e]$(\times 10^8)$	$\langle \phi \rangle$[f]
Pot	1.00	…	0.02	24°
Wh$^+$	1.03	0.24	7.4	24°
Tha	1.04	0.52	34.0	25°
Wh$^-$	1.18	0.16	1.9	27°
Val	1.04	0.26	71.0	28°
Am1$^-$	1.25	0.09	0.72	28°
Am2$^-$	1.22	0.12	1.7	28°
Can$^-$	1.24	0.09	1.6	28°
Wie	1.08	0.46	20.0	32°
McT	1.15	0.37	15.0	38°
Rég$^-$	1.04[g]	0.37	6.2	42°
Rég$^+$	0.87[g]	0.42	6.4	44°

DeRosa et al. (2009)

The misalignment angle between STEREO loops and potential field code is $\alpha_{mis}=24^0$, and for various NLFFF codes is $\alpha_{mis}=24^0-44^0$.

→ Potential field and NLFFF codes show a comparable discrepancy. The problems seems not to lie in the non-potentiality of the AR.

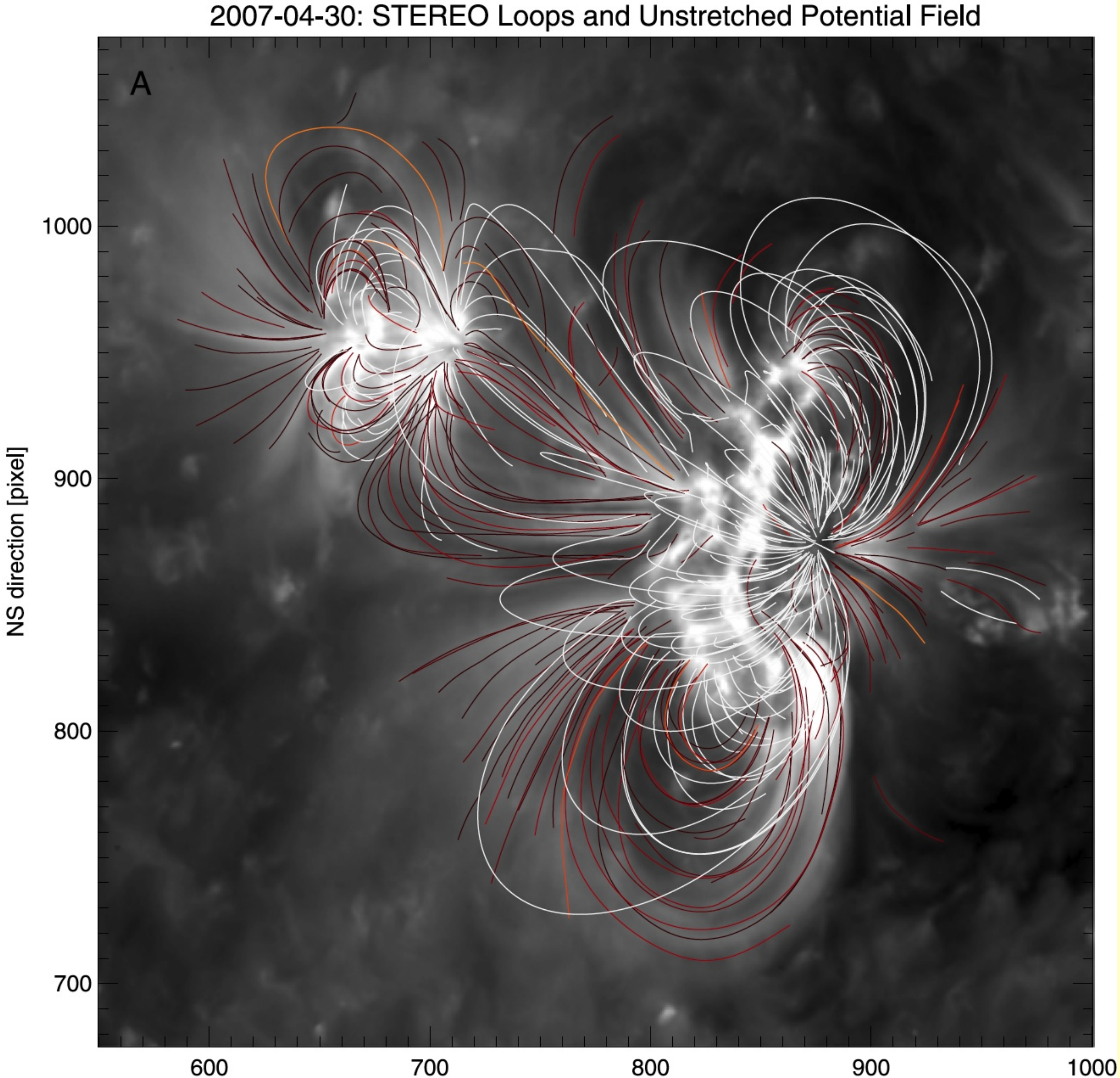

Misalignment:

<30^0 (brown)

~40^0 (red)

~60^0 (orange)

>70^0 (yellow)

Sandman
et al. (2009)

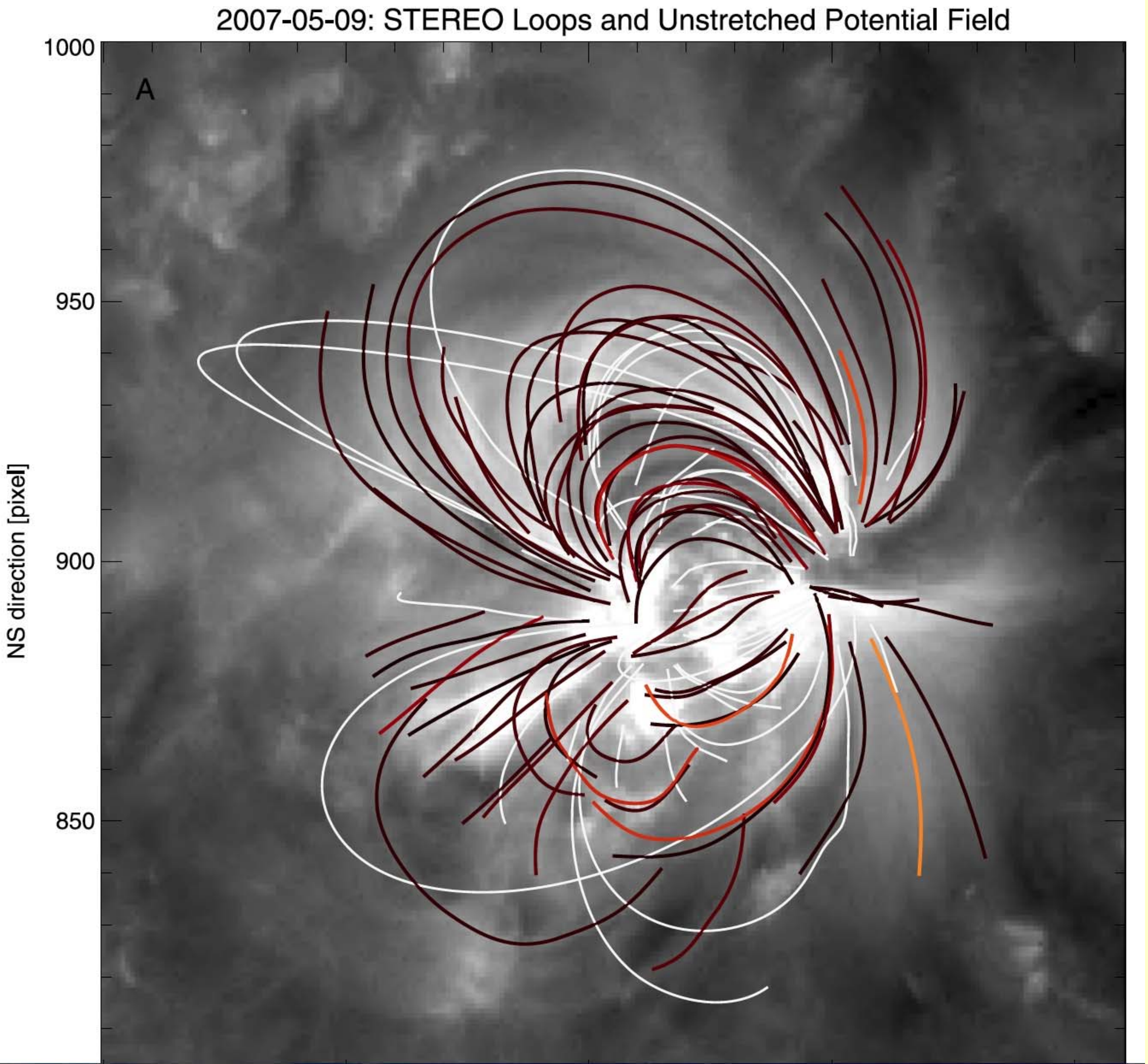

Misalignment:
$<30^0$ (brown)
$\sim 40^0$ (red)
$\sim 60^0$ (orange)
$>70^0$ (yellow)

Sandman
et al. (2009)

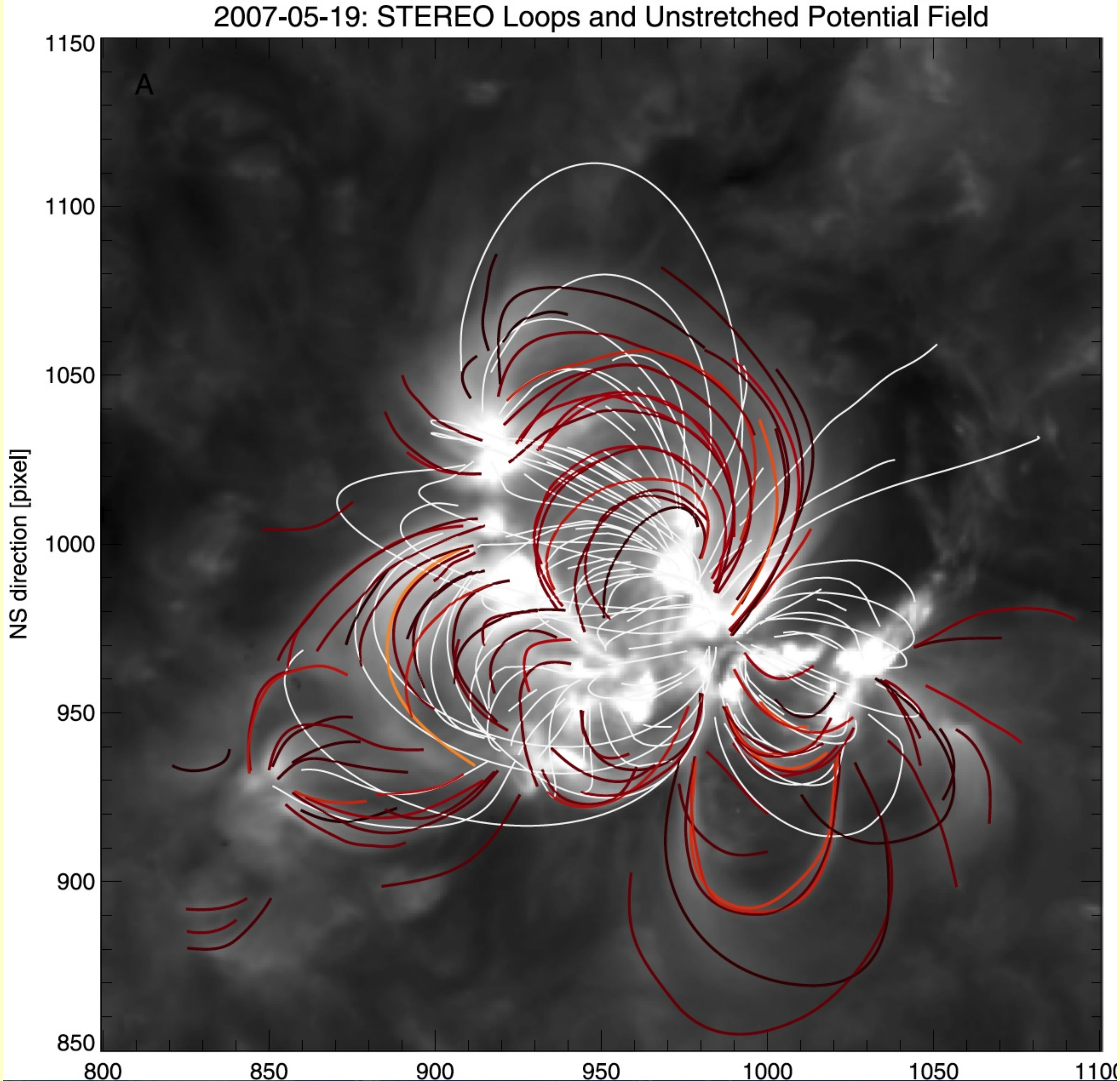

Misalignment:

$<30^0$ (brown)

$\sim40^0$ (red)

$\sim60^0$ (orange)

$>70^0$ (yellow)

Sandman
et al. (2009)

AR 10953, 2007-Apr-30 23:30 UT

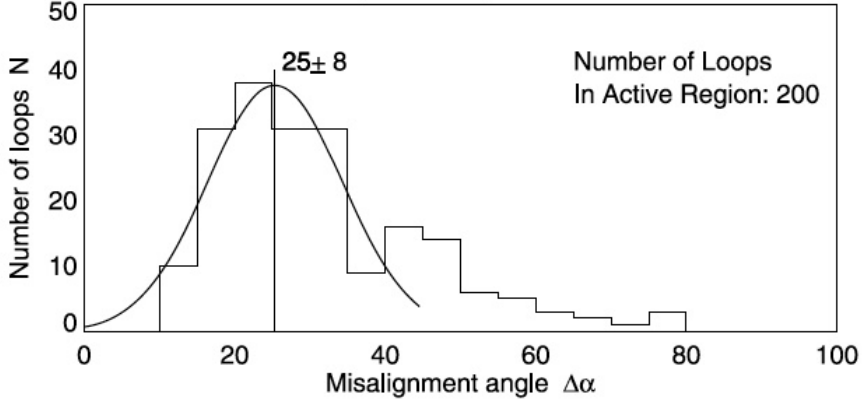

AR 10955, 2007-May-09 20:30 UT

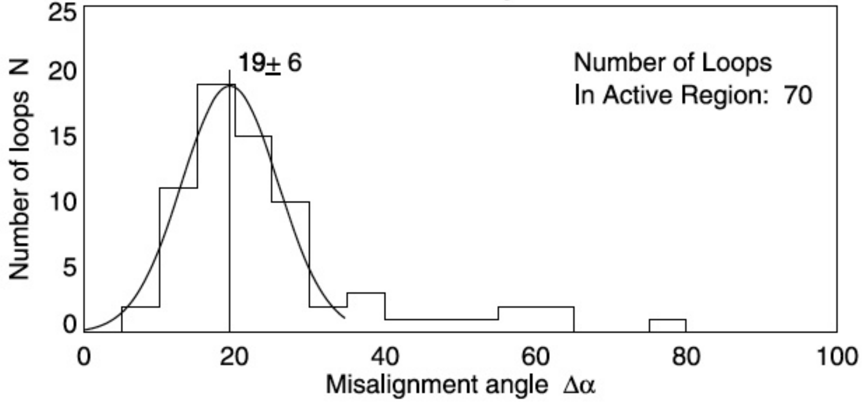

AR 10956, 2007-May-19 12:40 UT

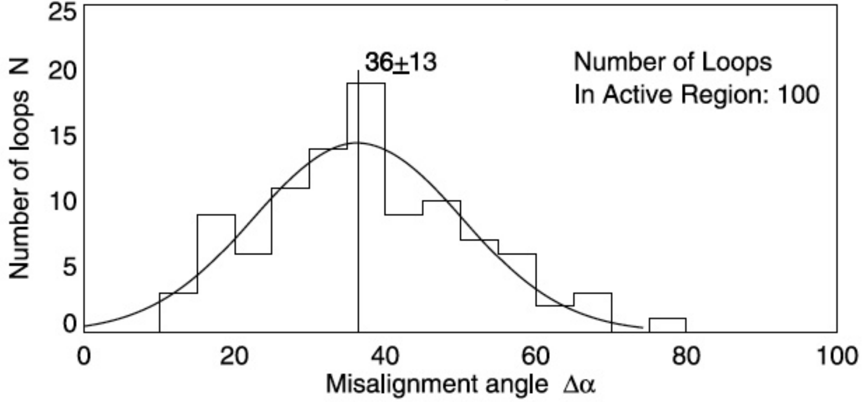

The average misalignment angle per loop (in 3D) ranges from ~20 deg for a very potential-like AR (2007 May 9) to ~40 deg for a flaring AR (2007 May 19).

The misaligments are commensurable for a Hinode FOV (DeRosa et al. 2009) and Full AR FOV (Sandman et al. 2009), for both potential field and nonlinear force-free (NLFF) field models.

Sandman
et al. (2009)

"The Usual Suspects" :

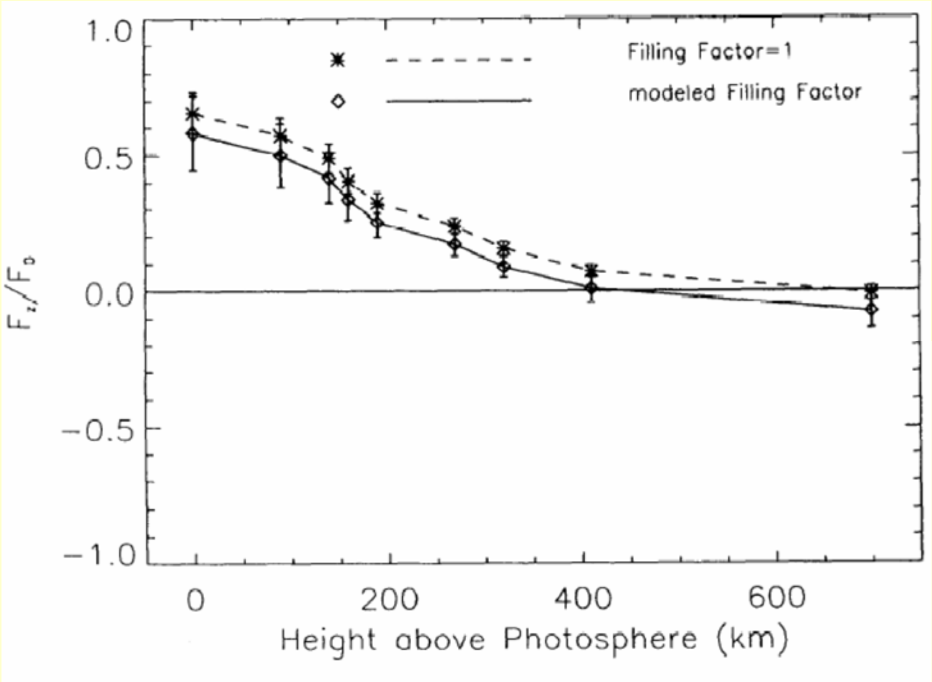

Metcalf et al. (1995)

Measurements of the net-Lorentz force in a force-free field using the virial theorem shows that the magnetic field becomes force free at heights of h>400 km above the photosphere (Metcalf et al. 1995).

Vector magnetograms sampling the photosphere, which is dynamic and contains Lorentz forces and buoyancy forces, do not provide a force-free boundary condition (DeRosa et al. 2009).

Non-Force-Free Magnetic Field Boundary

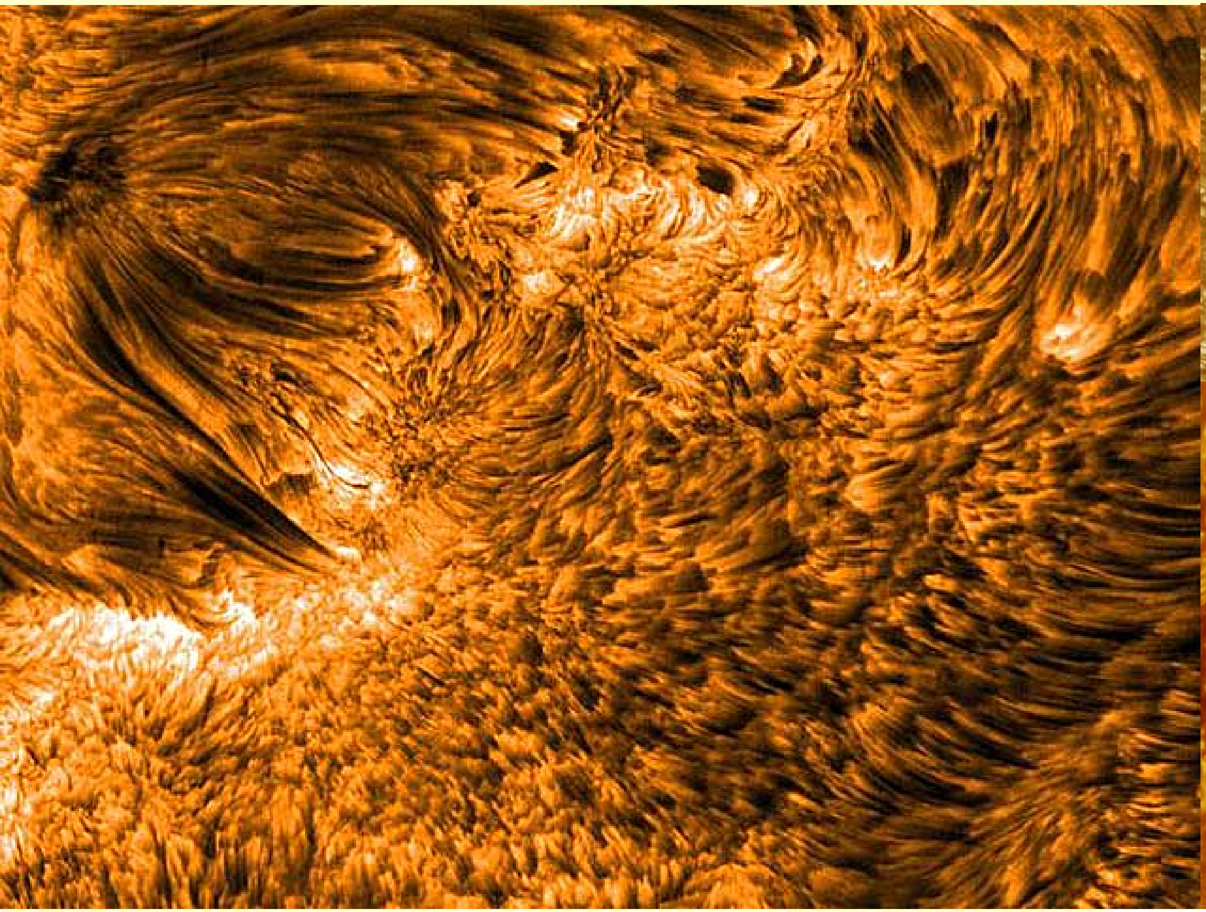

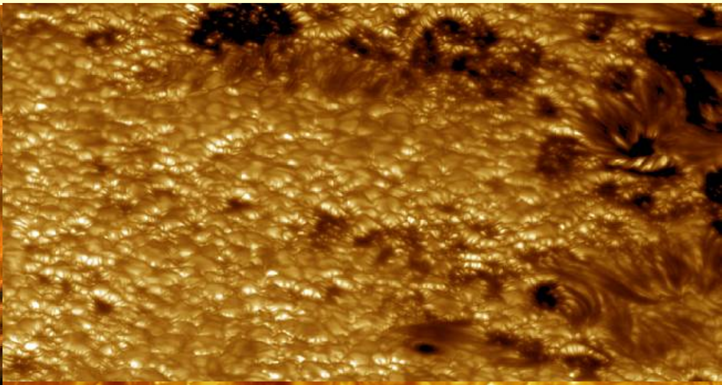

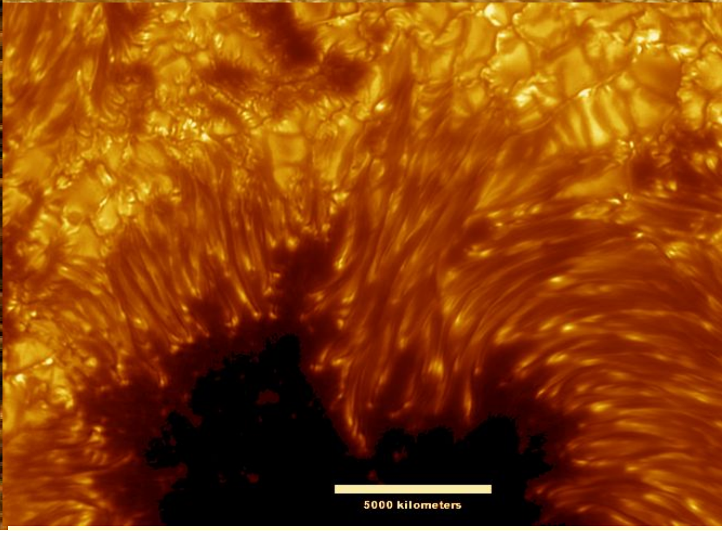

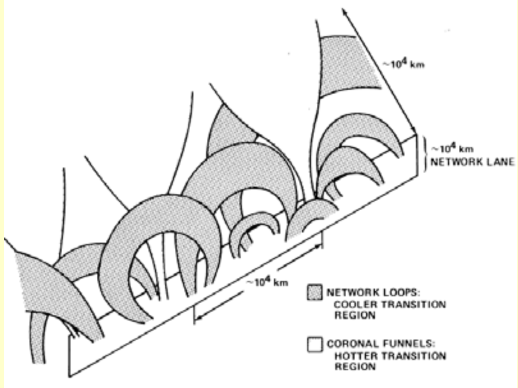

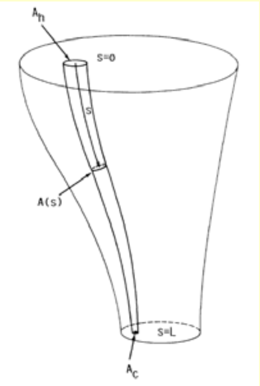

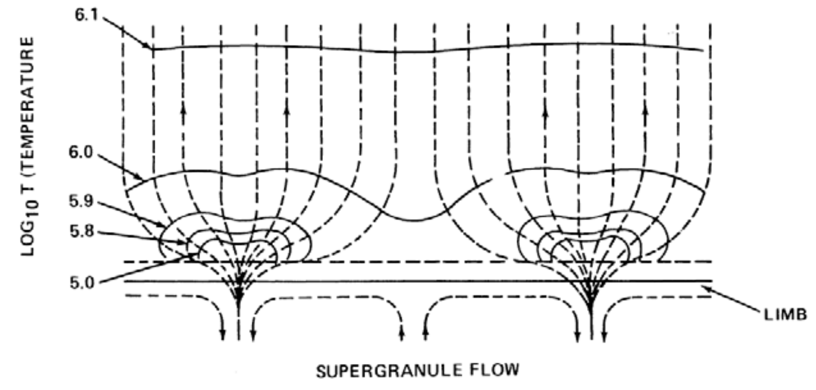

Dynamic fibrils, mottles, spicules

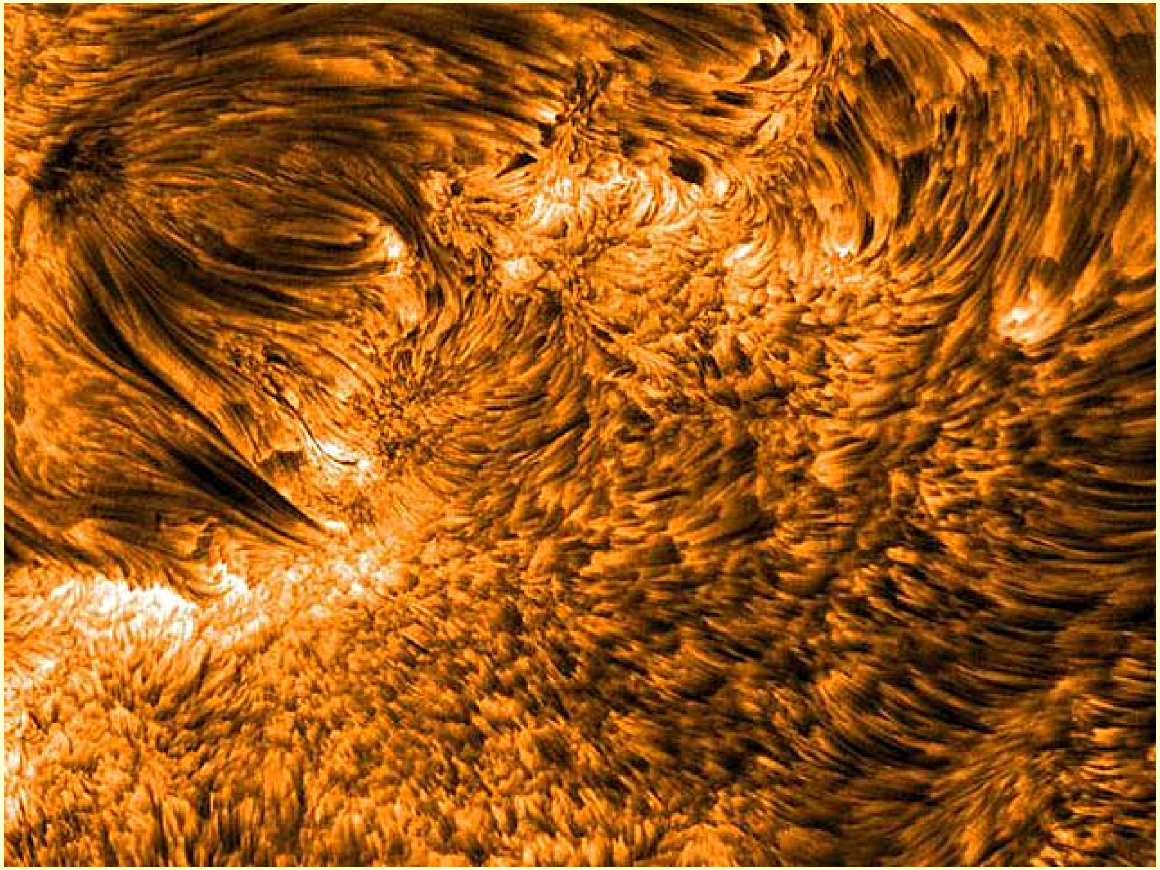

Swedish 1-m Solar Telescope at La Palma, Spain

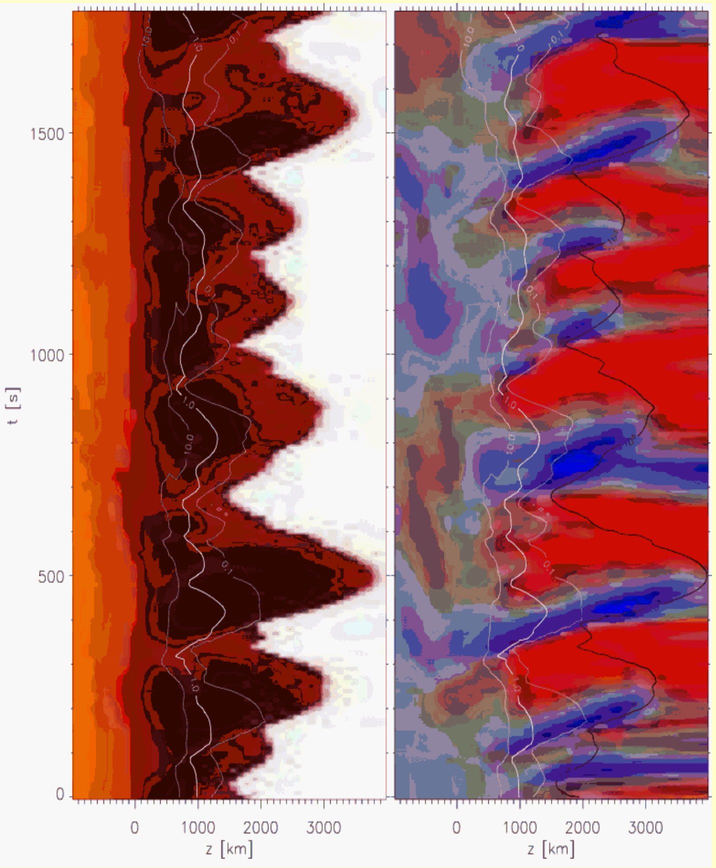

DePontieu et al. (2007, ApJ 655, 624)

High-resolution Hα images reveal for the first time, spatially and temporally resolved dynamic fibrils in active regions. These jet-like features are similar to mottles or spicules in the quiet-Sun. Their 3D structure can be reconstructed from the parabolic path trajectory of chromospheric shock waves, which can be reproduced by radiative MHD simulations (right frame).

Extrapolating the Magnetic Field into the Corona

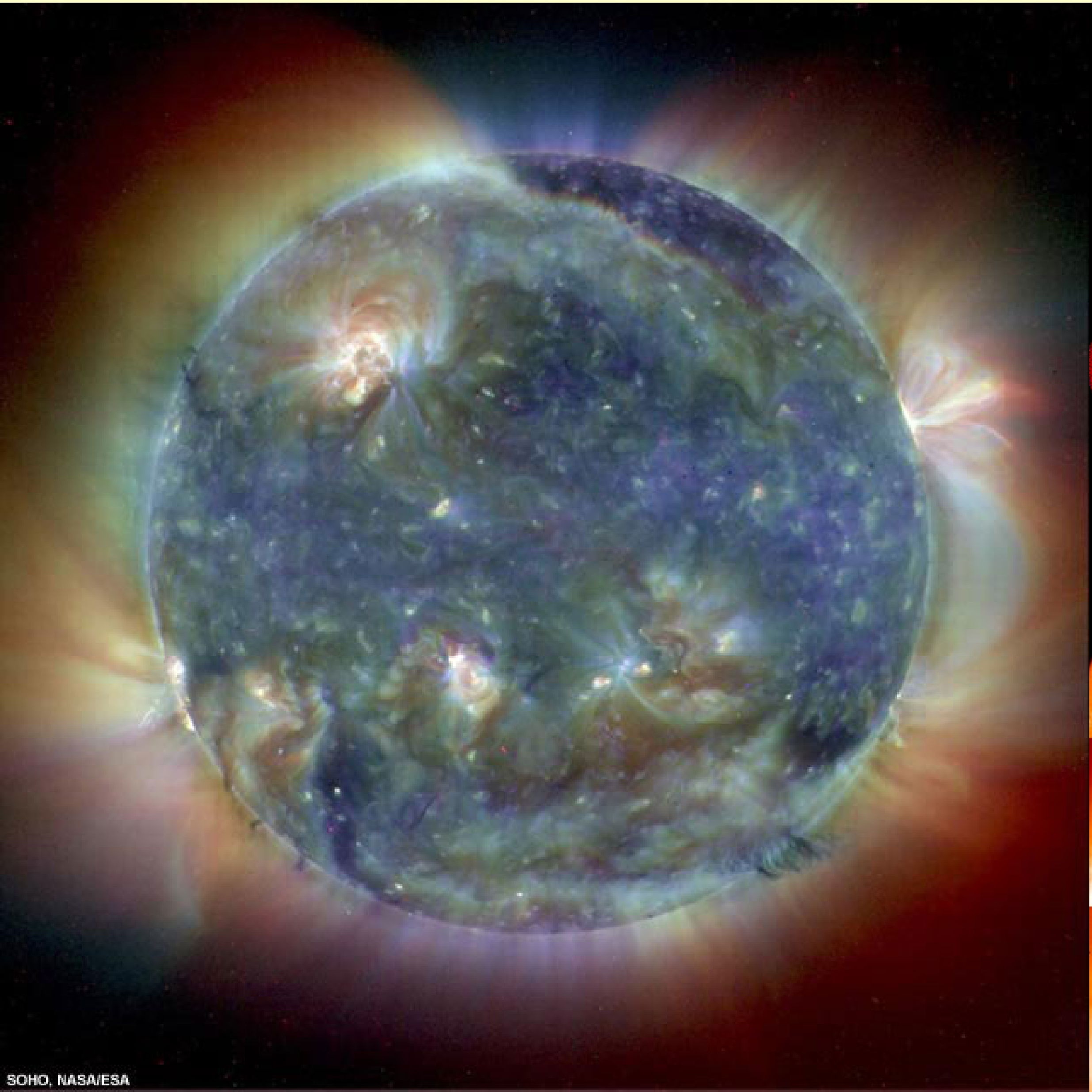

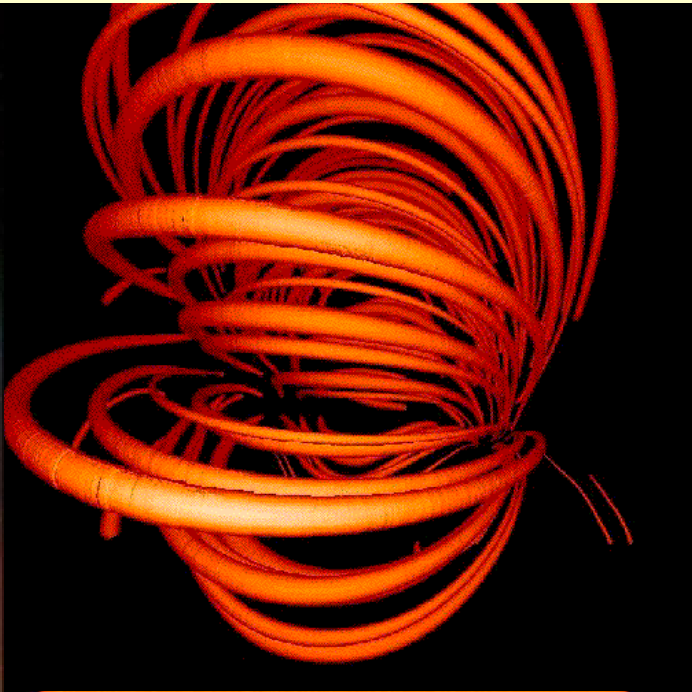

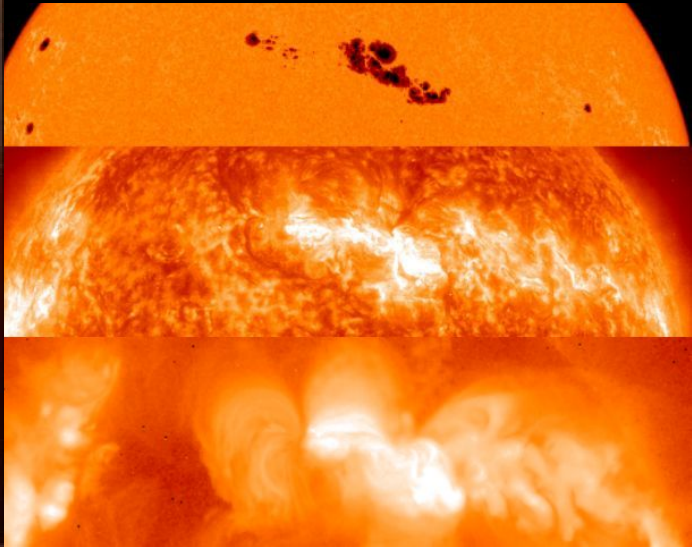

Stereoscopic 3-D Reconstruction of Coronal Loops

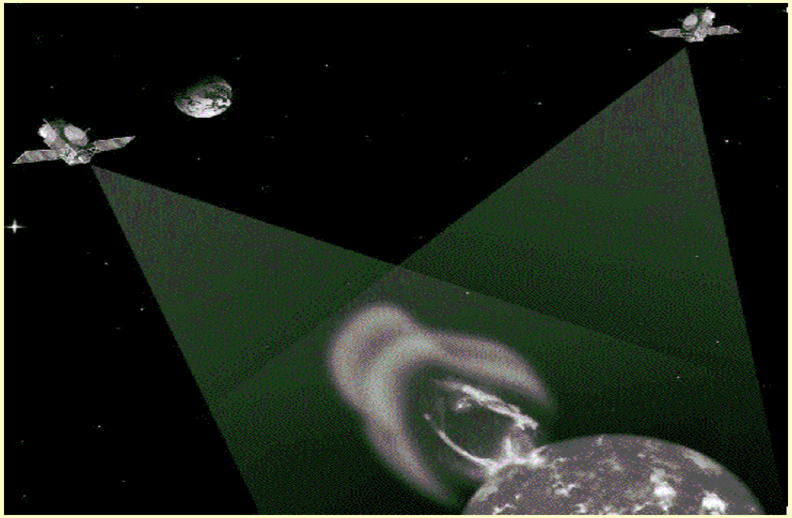

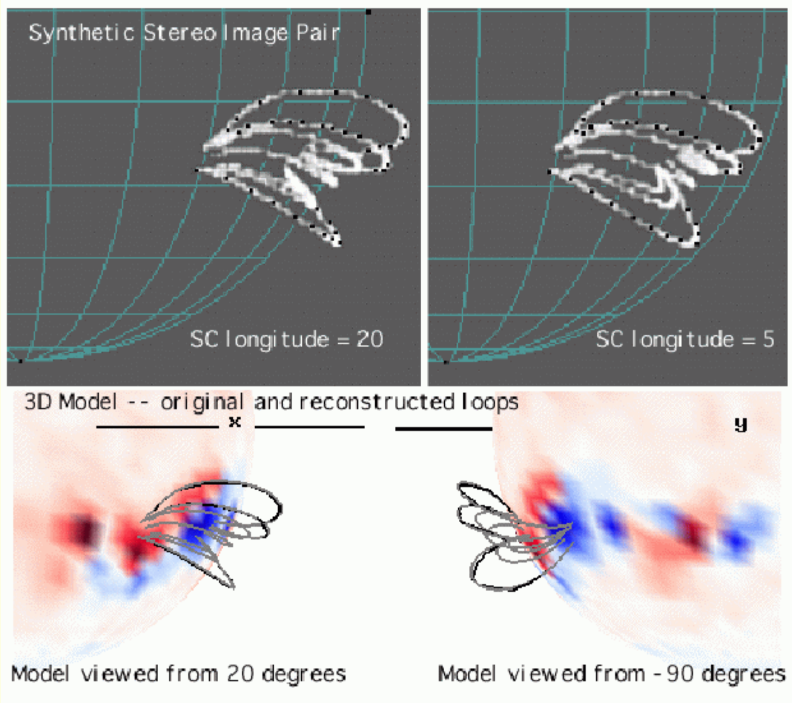

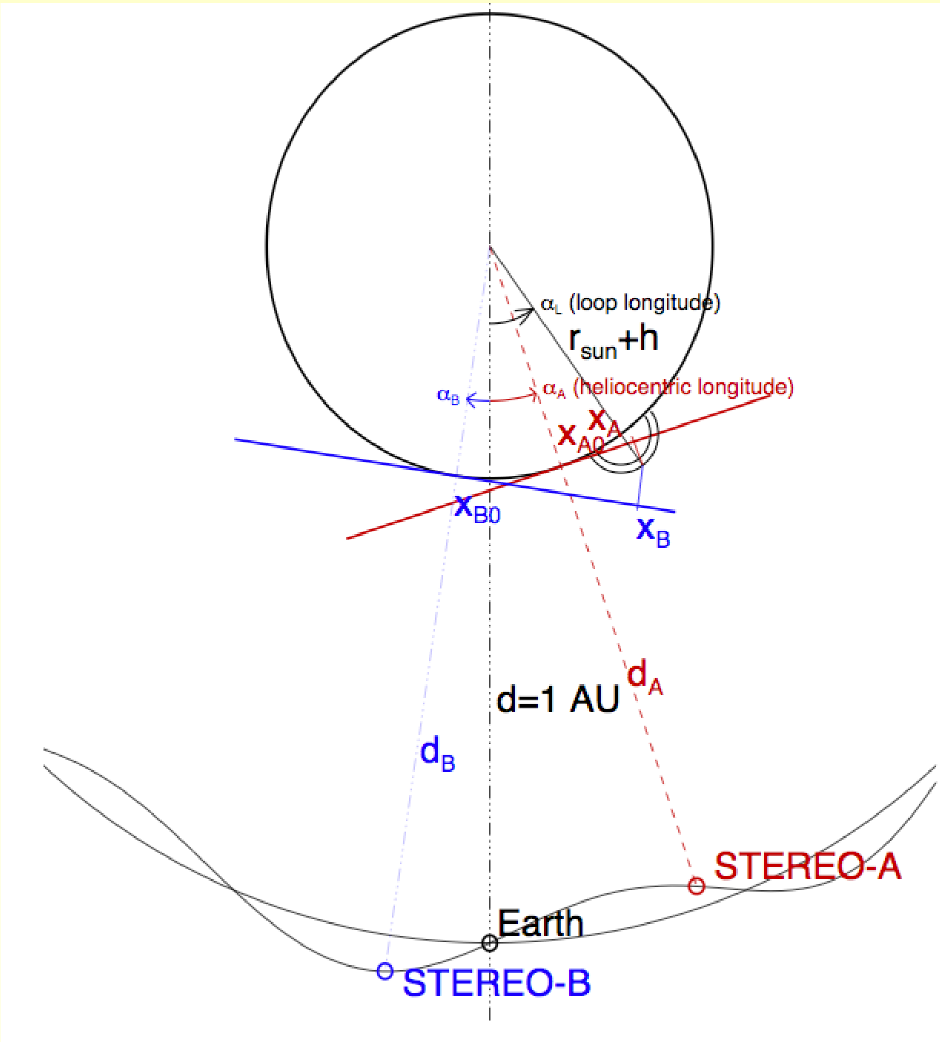

The method of two-spacecraft stereoscopy became feasible since the launch of STEREO A(head) and B(ehind) (Oct 2006).

Stereoscopic image pair and highpass filtering

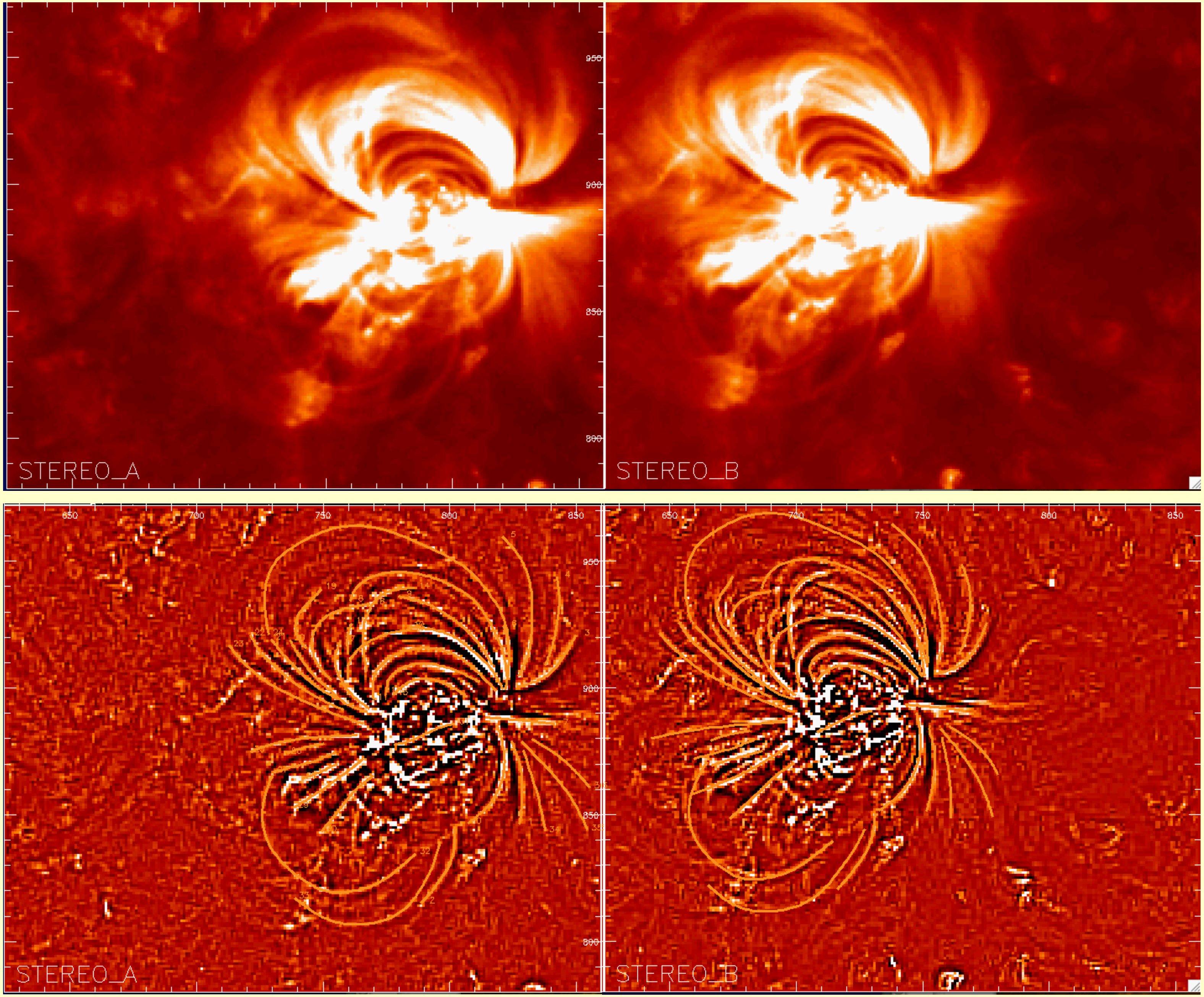

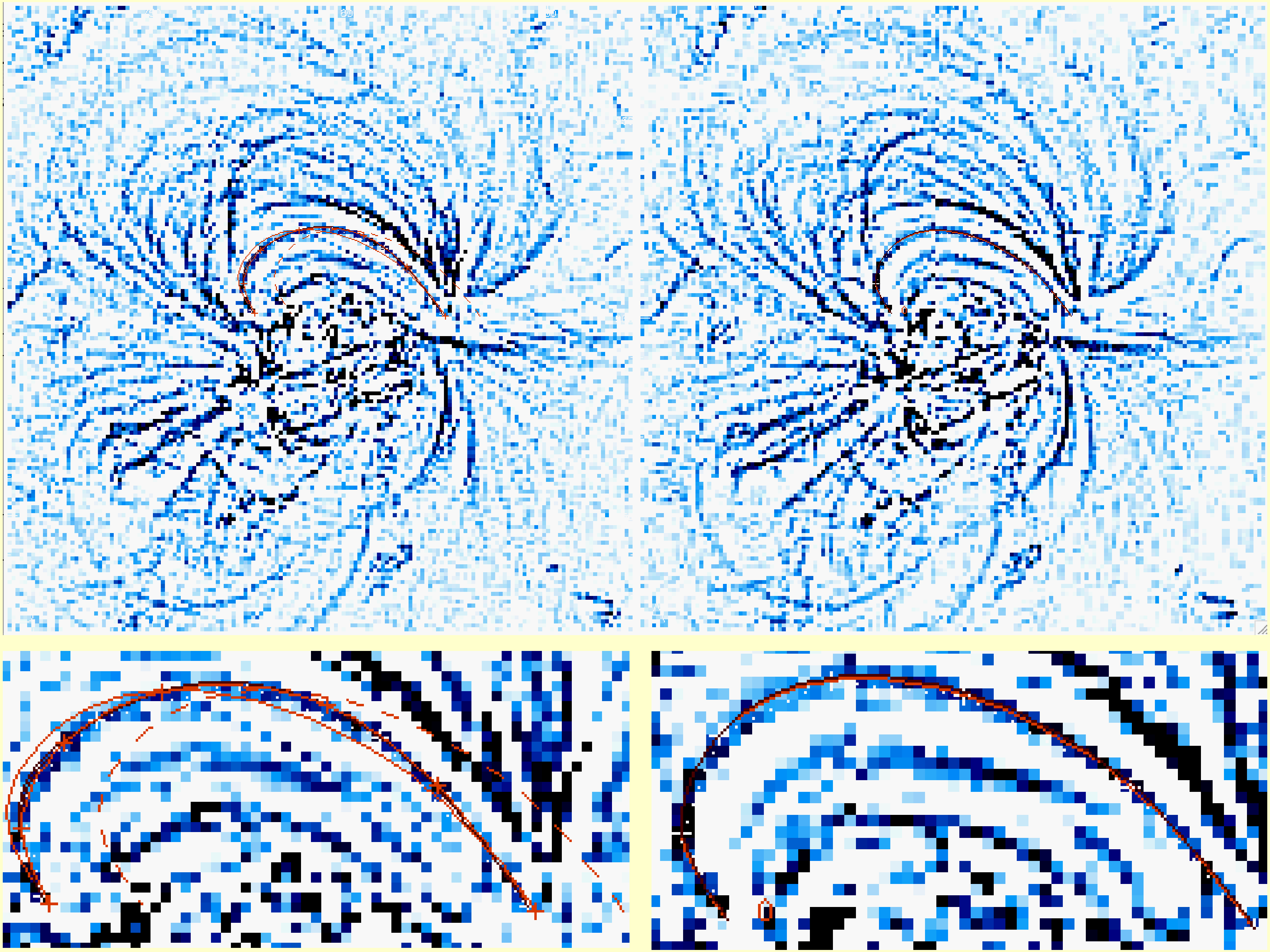

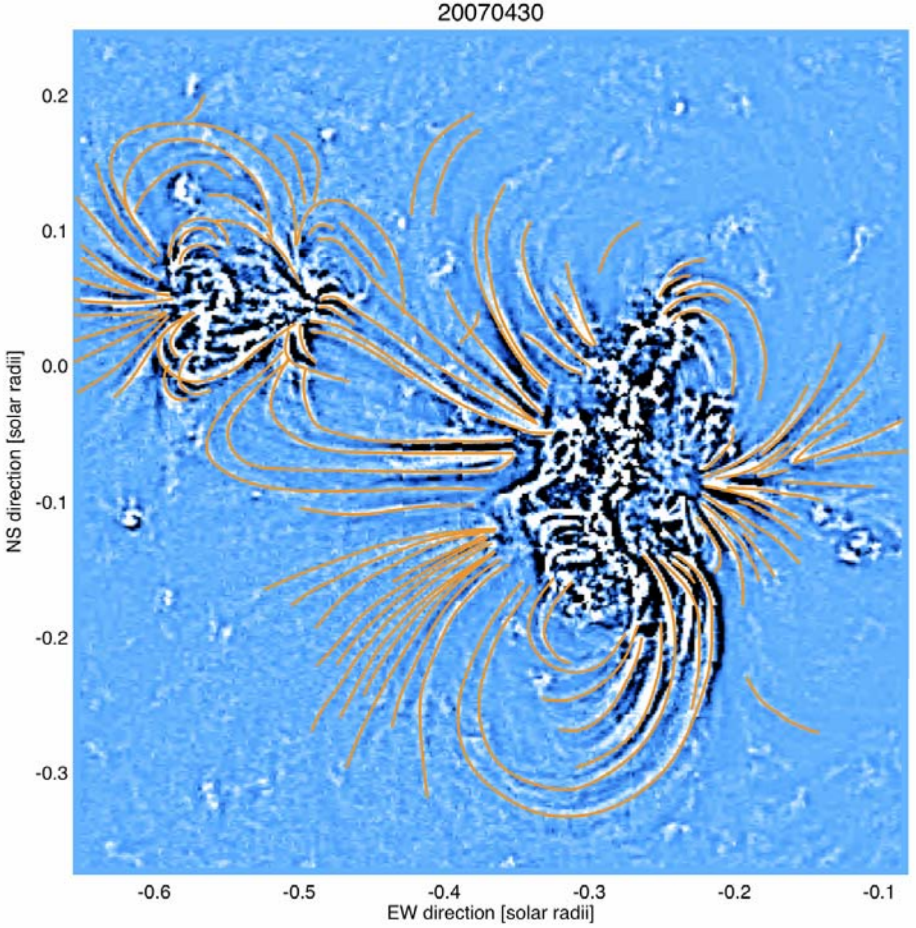
20070430

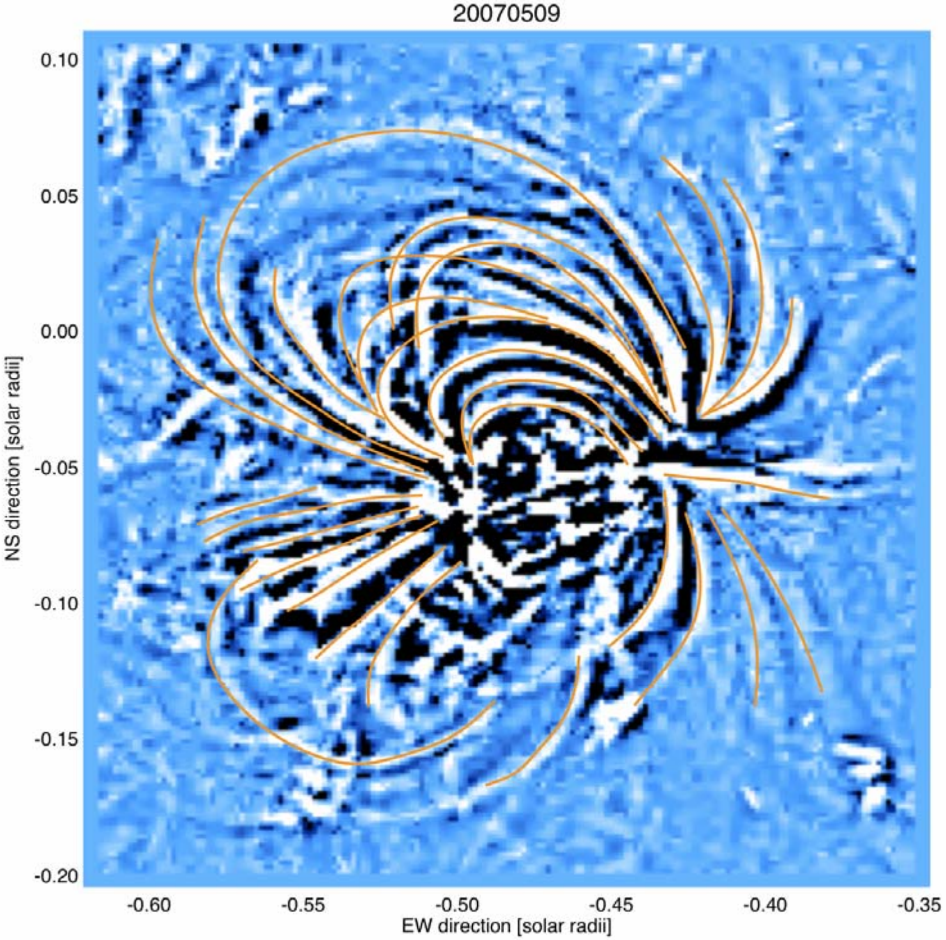
20070509

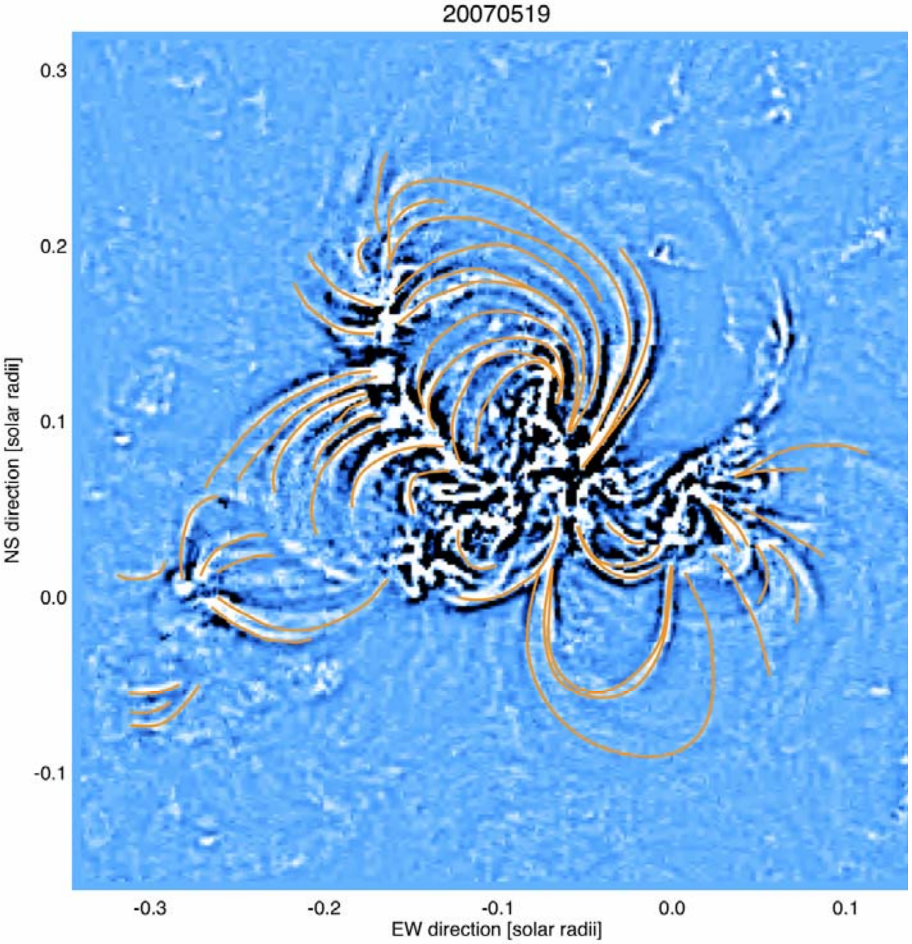
20070519
NS direction [solar radii]
0.3
0.2
0.1
0.0
-0.1
-0.3
-0.2
-0.1
0.0
0.1
EW direction [solar radii]

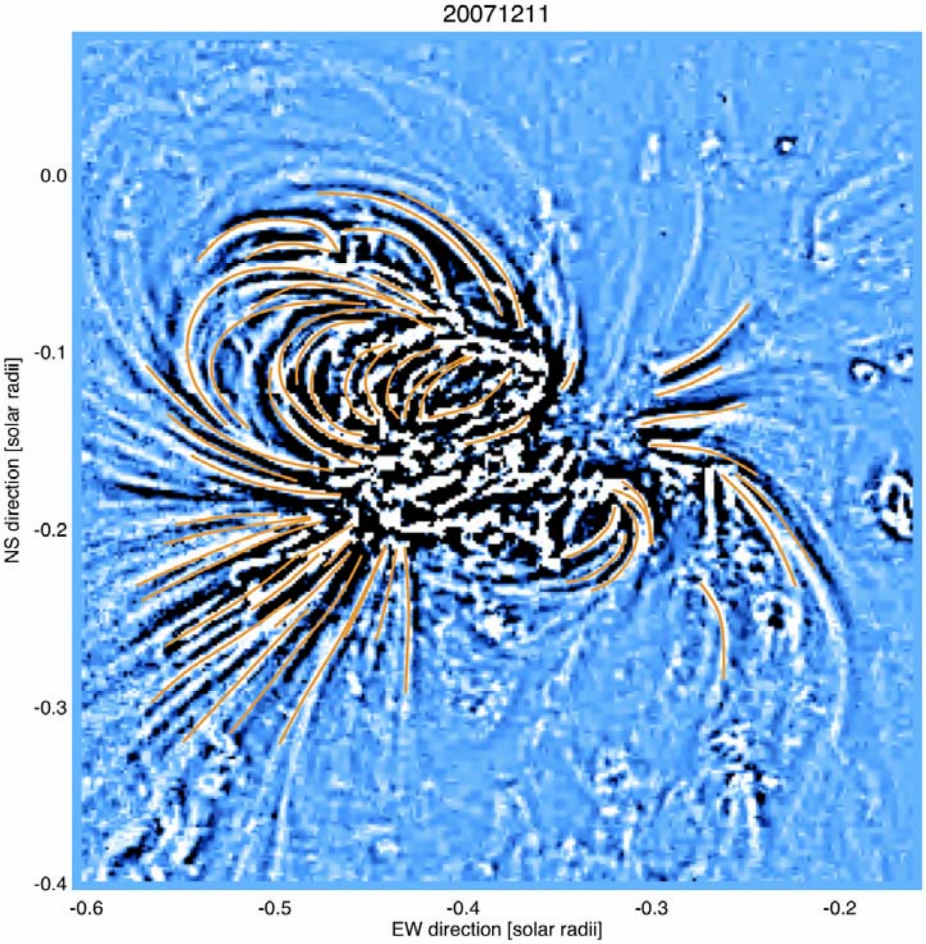
20071211
NS direction [solar radii]
0.0
-0.1
-0.2
-0.3
-0.4
-0.6
-0.5
-0.4
-0.3
-0.2
EW direction [solar radii]

Stereoscopic triangulation of EUVI triple-filter images

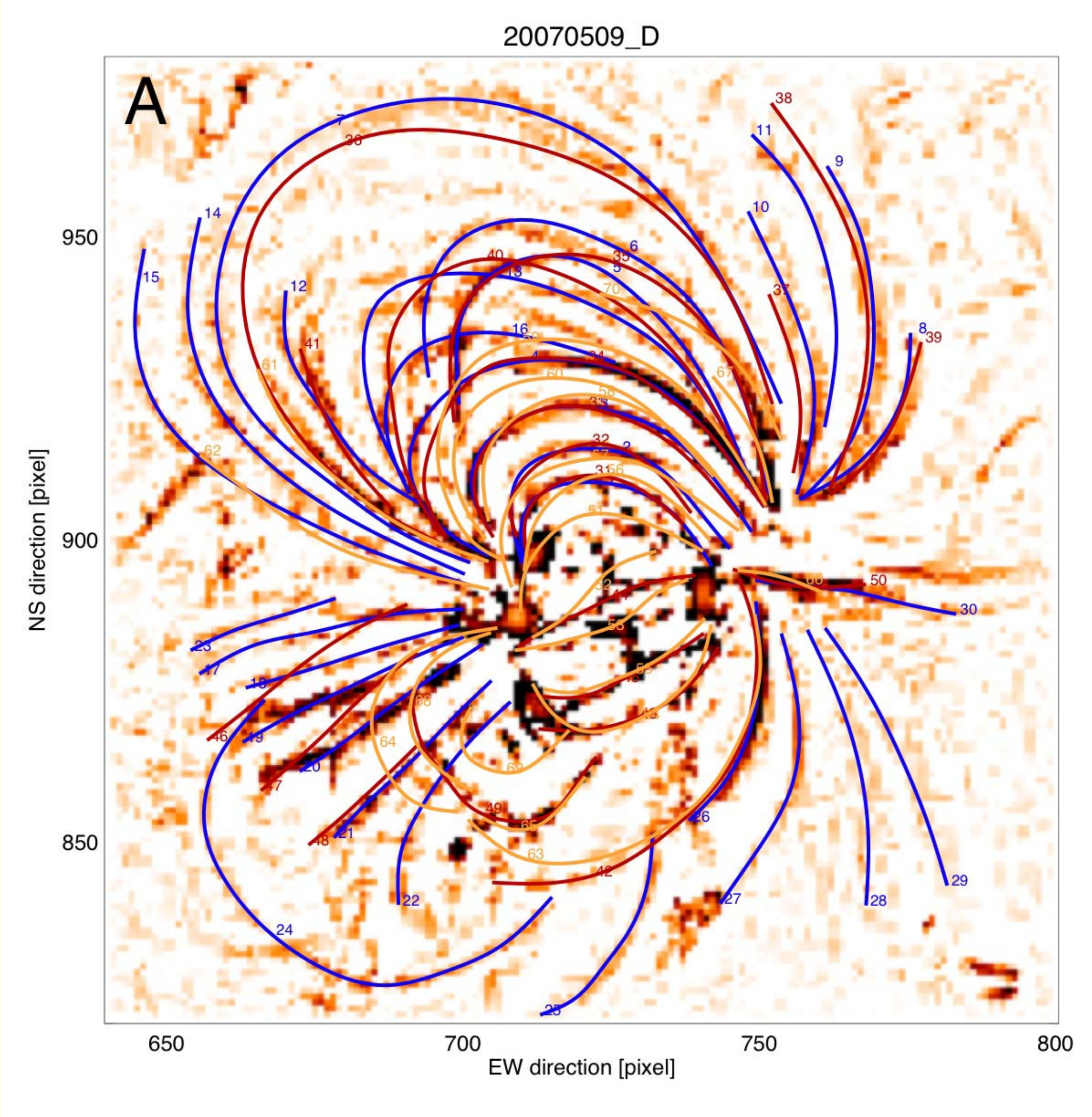

171 A
195 A
284 A

Aschwanden et al. (2008a,b; 2009)

3D Reconstruction of 100 loops (T=1.0-2.0 MK)

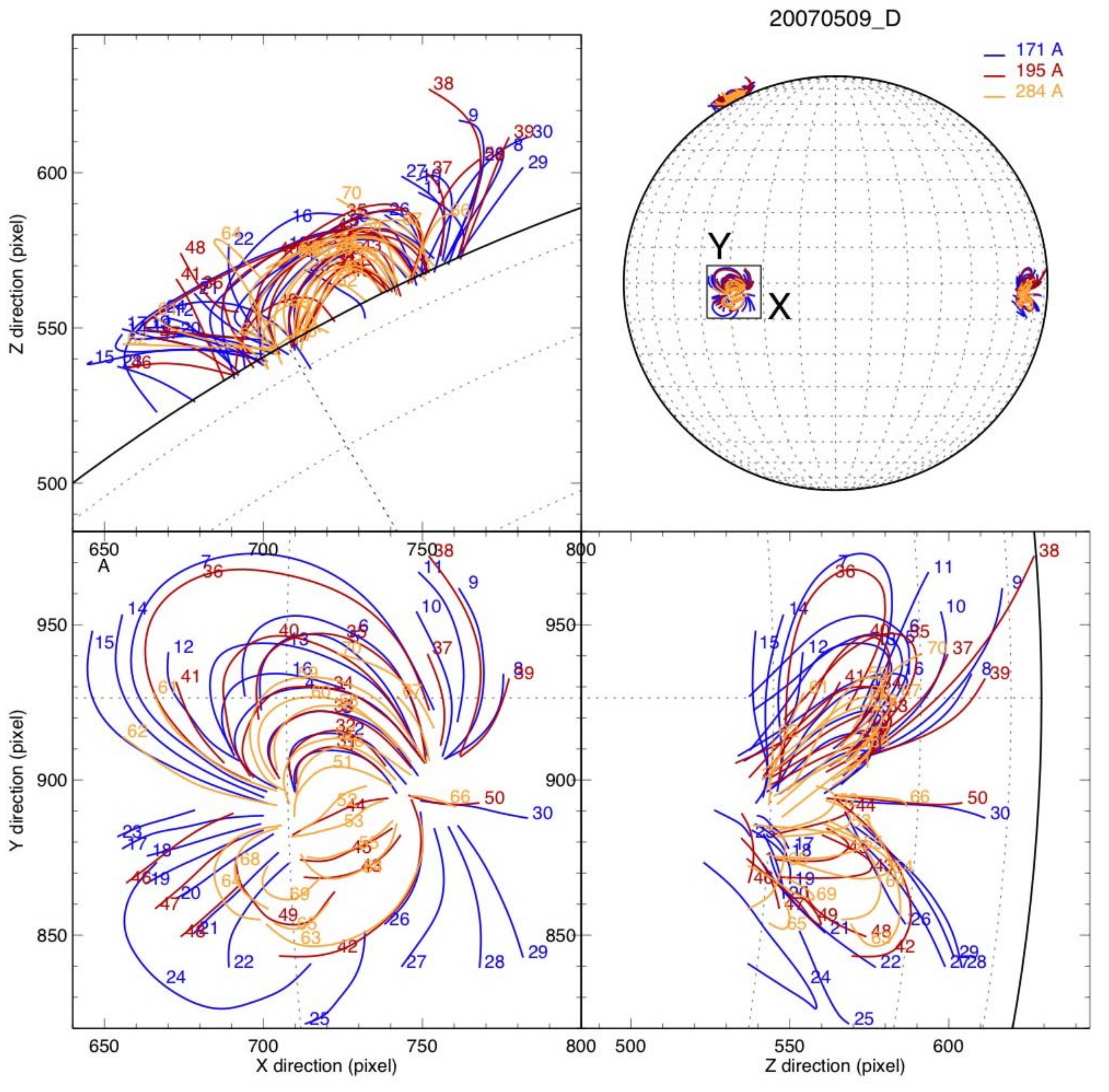

Bootstrapping Method of Coronal Magnetic Field

Stereoscopically triangulated loops provide the correct 3D field directions (in dimensionless units) along a set of loops:

$$b(s) = \frac{B(s)}{|B(s)|} = \frac{[B_x(s), B_y(s), B_z(s)]}{|B(s)|}$$

A physical solution of the magnetic field needs to fulfill Maxwell's equation of a divergence-free field:

$$\nabla B = \left(\frac{\partial B_x}{\partial x}, \frac{\partial B_y}{\partial y}, \frac{\partial B_z}{\partial z} \right) = 0$$

Abelian properties of divergence-free field:

$$\nabla (A + B) = \nabla A + \nabla B$$

$$\nabla B = \nabla (\pm cb) = \pm c \bullet \nabla b$$

Potential field of a unipolar magnetic charge:

$$\Phi(r) = -\Phi_0 \left(\frac{z_0}{r} \right),$$

$$B_r(r) = \nabla\Phi(r) = B_0 \left(\frac{z_0}{r} \right)^2,$$

$$\Delta\Phi(r) = \nabla B(r) = \frac{1}{r^2} \frac{\partial}{\partial r} \left(r^2 \frac{\partial\Phi(r)}{\partial r} \right) = 0.$$

A potential field B(x,y,z) can be represented by a superposition of multiple unipolar magnetic charges:

$$B(x) = \sum_{i=1}^{n} B_i(x) = \sum_{i=1}^{n} B_i \left(\frac{z_i}{r_i} \right)^2 \frac{r_i}{|r_i|},$$

$$r_i = [(x - x_i)^2 + (y - y_i)^2 + (z - z_i)^2]^{1/2}$$

This parameterized B-field (with 4n parameters B_i, x_i, y_i, z_i) can be forward-fitted to STEREO field lines b=B/|B|.

Schematic Representation of the Parametric Transformation Analysis (PTA)

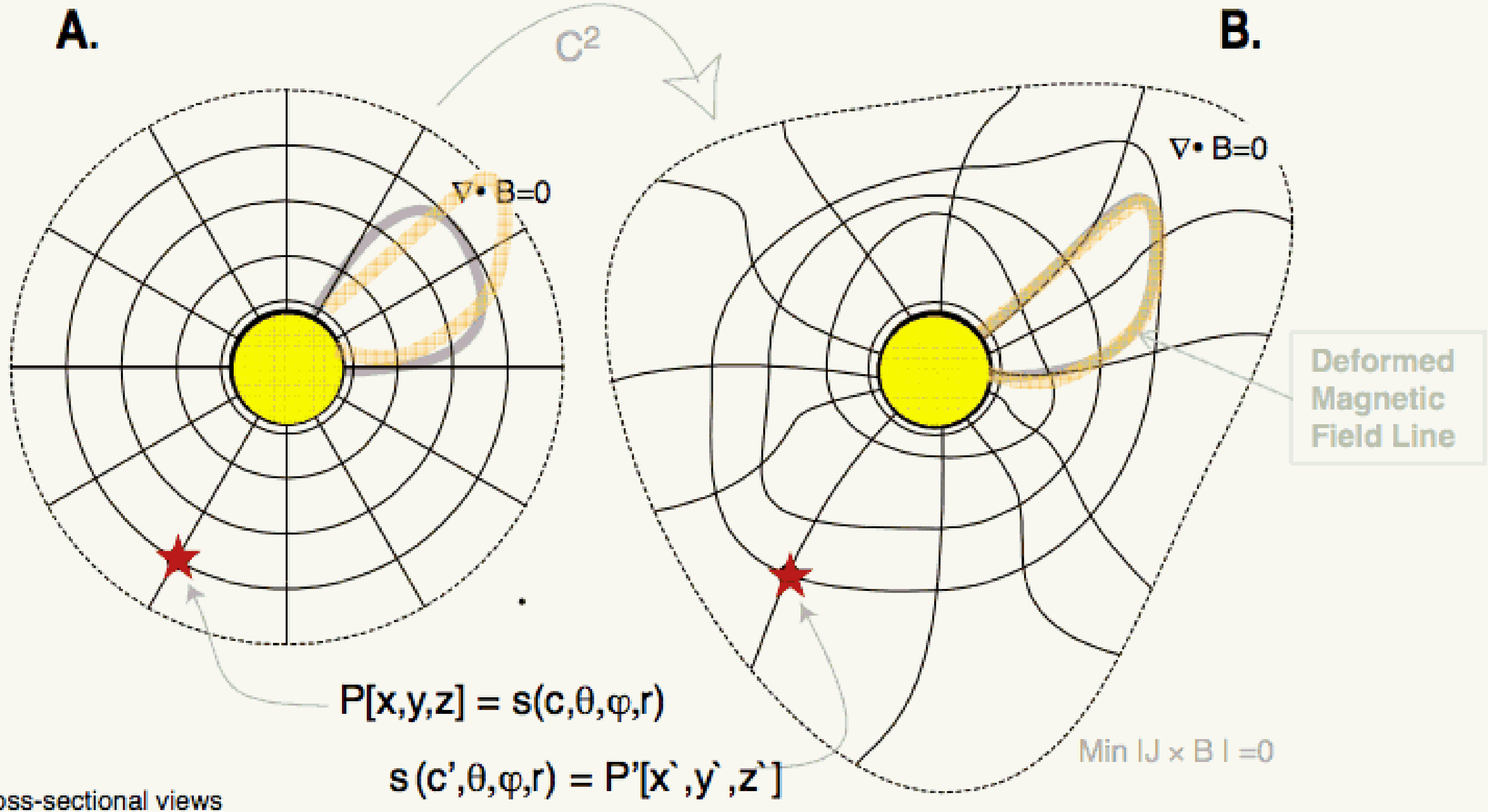

Cross-sectional views

- The "coronal" coordinate space points (∈ field lines) X[x,y,z] are transformed into X'[x',y',z'].
- The magnetic field is transformed into another magnetic field solution: $B' = J\,B / \det(J)$
- The new solution is divergent free: the transformed field has C^2 continuity.

Uniqueness constraints:

(i) The photospheric magnetic vector field

(ii) The field satisfies the observed coronal loop structure

(iii) The magnetic field minimizes the Lorentz forces in the volume

PTA conserves initial model topology, i.e., does not employ reconnection

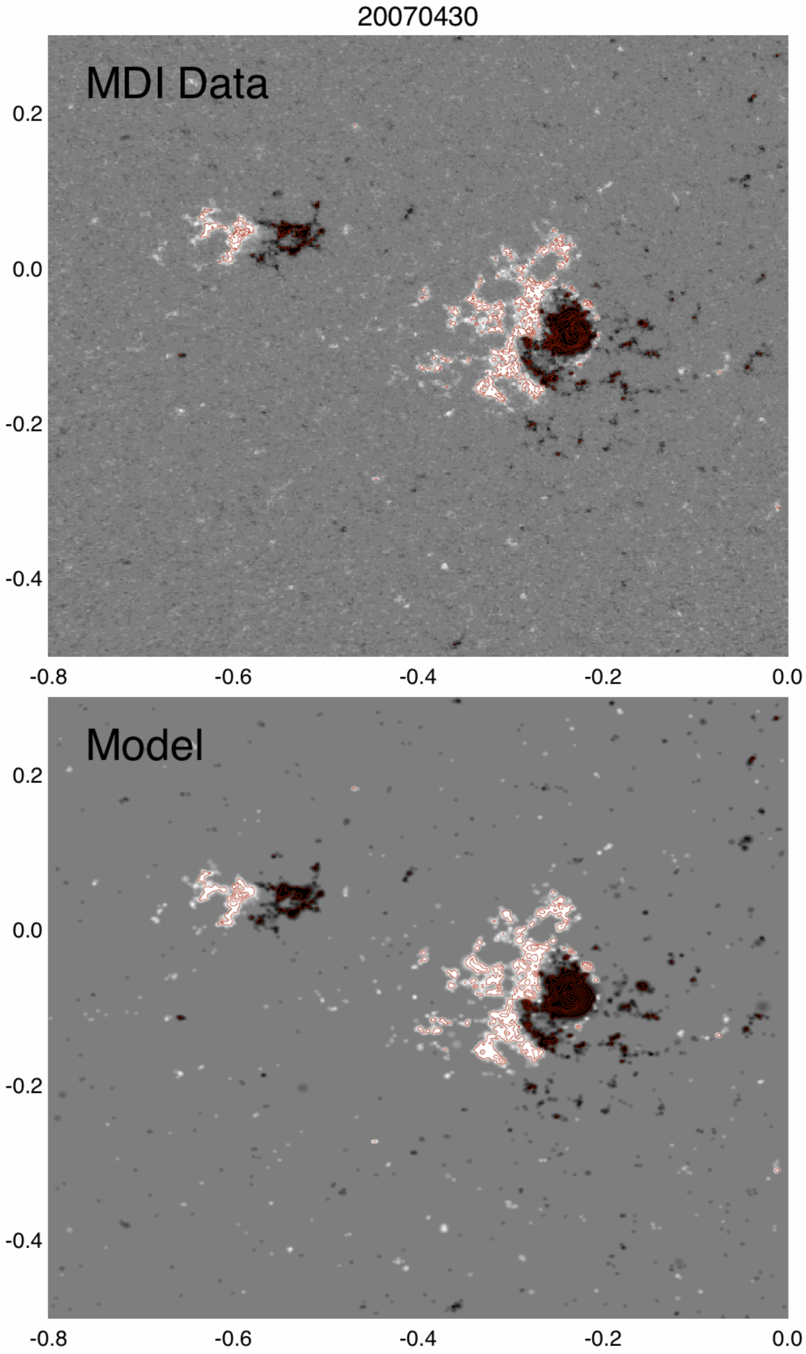

Observed MDI magnetogram rotated into same field-of-view as STEREO/A

Decomposition of MDI magnetogram into n=2000 unipolar magnetic charges by fitting 2D gaussians and determining depth $z_i=w_i$ from width w_i=FWHM/2 (→8000 coefficients B_i,x_i,y_i,z_i).

Misalignment angle definition

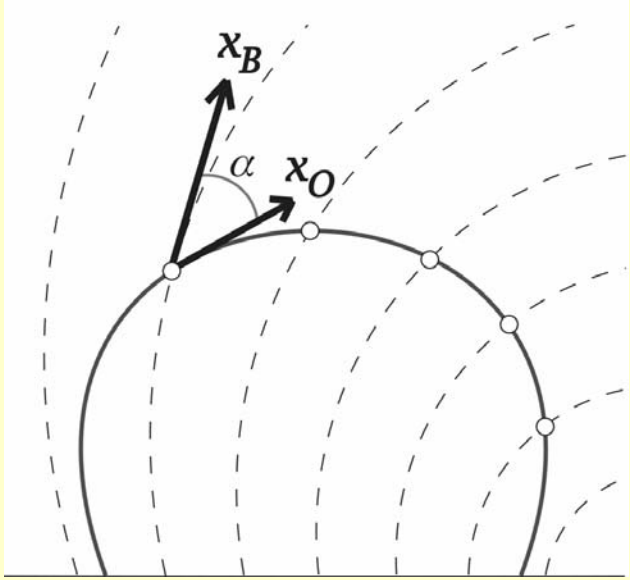

The misalignment angle α_{mis} is defined in 3D between the direction of a stereoscopically triangulated loop direction (x_O) and the field vector (x_B) of a theoretical magnetic field model, averaged over n positions along a loop.

$$\alpha_{mis}(x,y,z) = \cos^{-1}\left(\frac{B_{theo}(x,y,z) \bullet B_{obs}(x,y,z)}{|B_{theo}(x,y,z| \bullet |B_{obs}(x,y,z)|} \right),$$

$$< \alpha_{mis}(x,y,z) >= \left[\frac{1}{n} \sum_{i=1}^{n} \alpha^2{}_{mis}(x,y,z) \right]^{1/2}$$

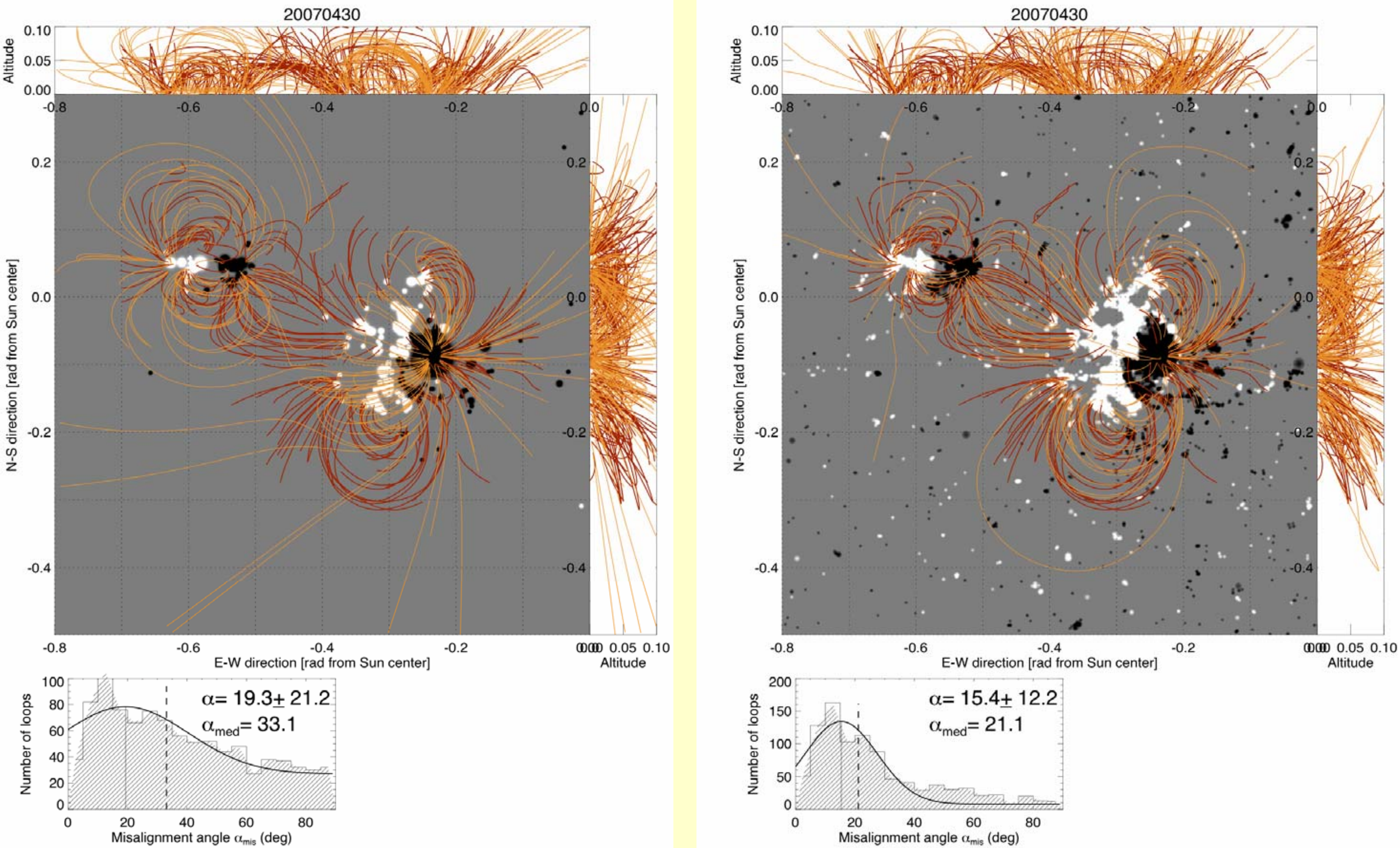

Magnetic field : 200 unipolar charges ←→ 2000 unipolar charges

The accuracy of the potential field model depends on the spatial and magnetic flux resolution

The median misalignment angle reduces from 33^0 to 21^0.

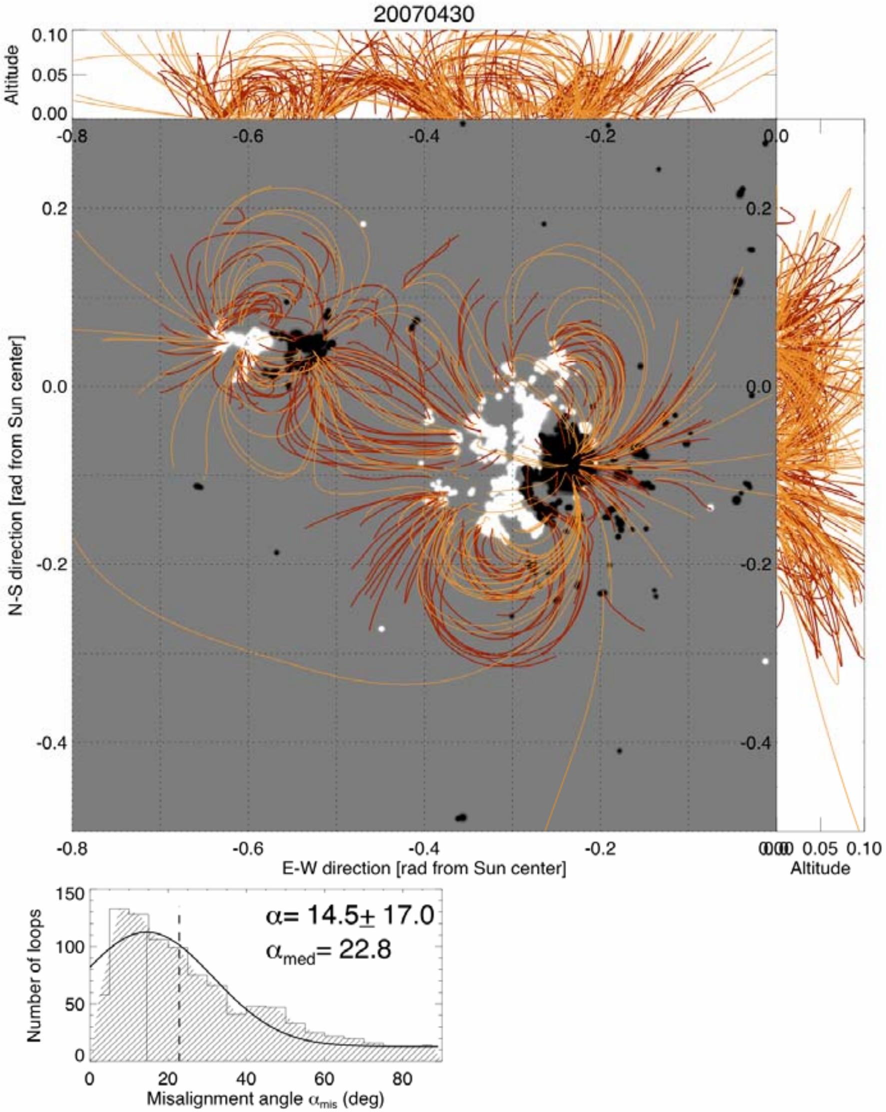

500 unipolar components
extrapolation without fitting
misalignment a=14.5+17.0

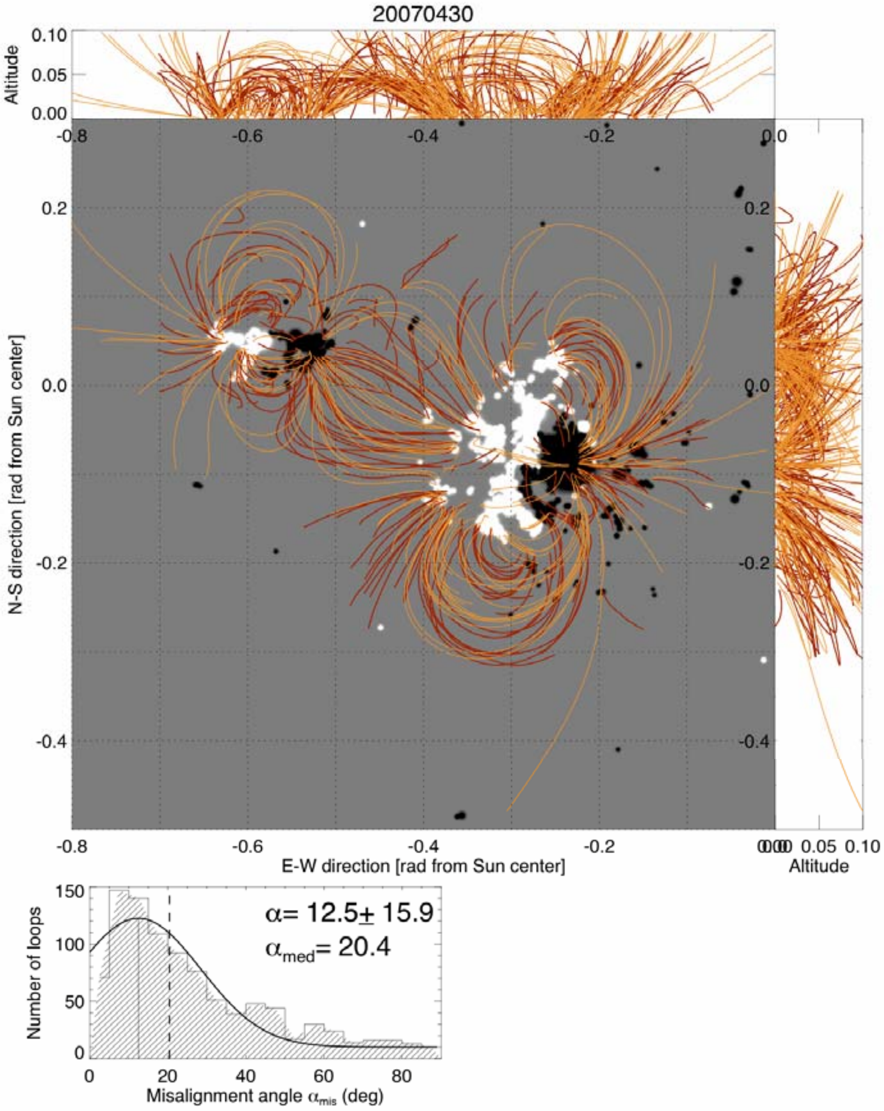

500 unipolar components
fitting 8 zones with variable B:
misalignment a=12.5+15.9

Comparison of misalignment angles For AR 10953 (2007 Apr 30, 23 UT)

PFSS code:

Sandman et al. 2009: a = 25 + 8 deg

DeRosa et al. 2009: a = 24 deg

NLFFF codes:

DeRosa et al. 2009: a = 24…44 deg

Unipolar Potential Field:

n=200 a = 19.3+21.2 deg

n=500 a = 14.5+17.0 deg

n=1000 a = 14.7+13.2 deg

n=2000 a = 15.4+12.2 deg

Unipolar Potential Field Fitting:

n=200 a = 14.0+12.7 deg

n=500 a = 12.5+15.9 deg

n=1000 a = 14.4+ 9.8 deg

Dipole Potential Field Fitting:

n=5 a = 16.4+ 7.8 deg

n=10 a = 17.4+ 9.7 deg

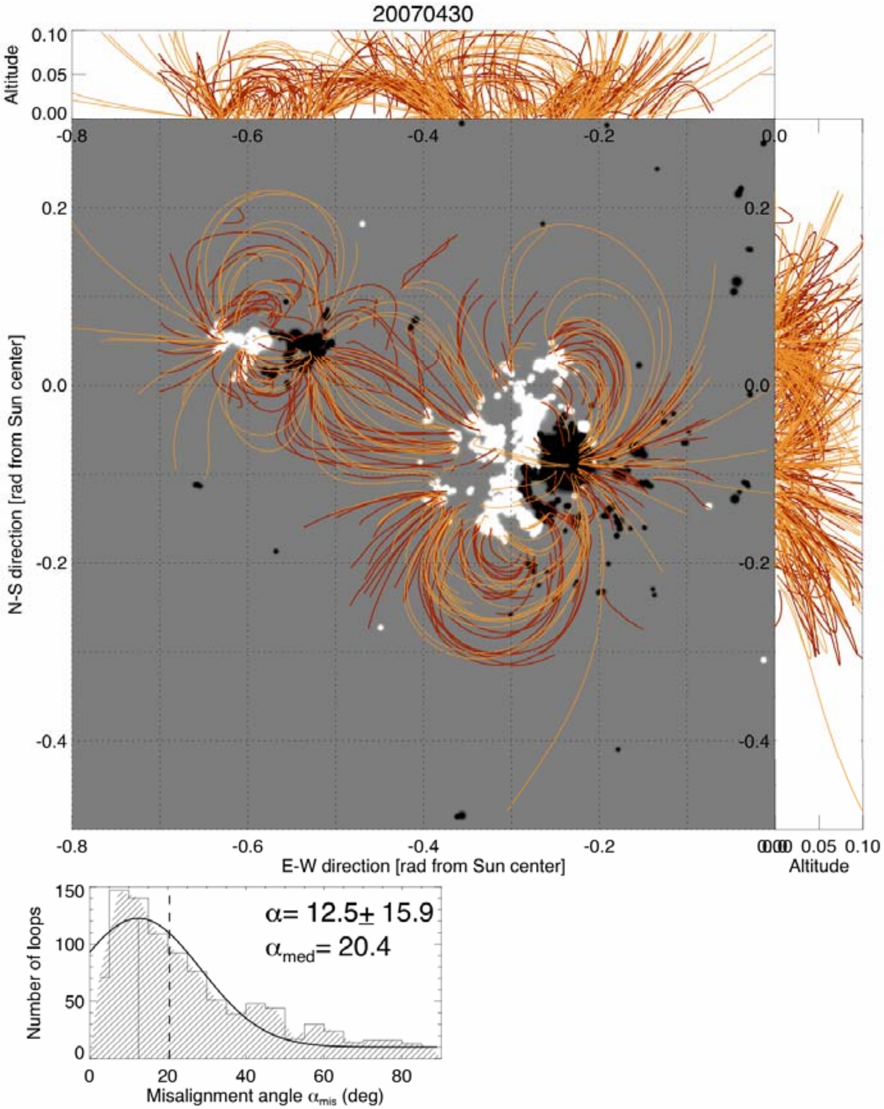

500 unipolar components fitting 8 zones with variable B: misalignment a=12.5+15.9

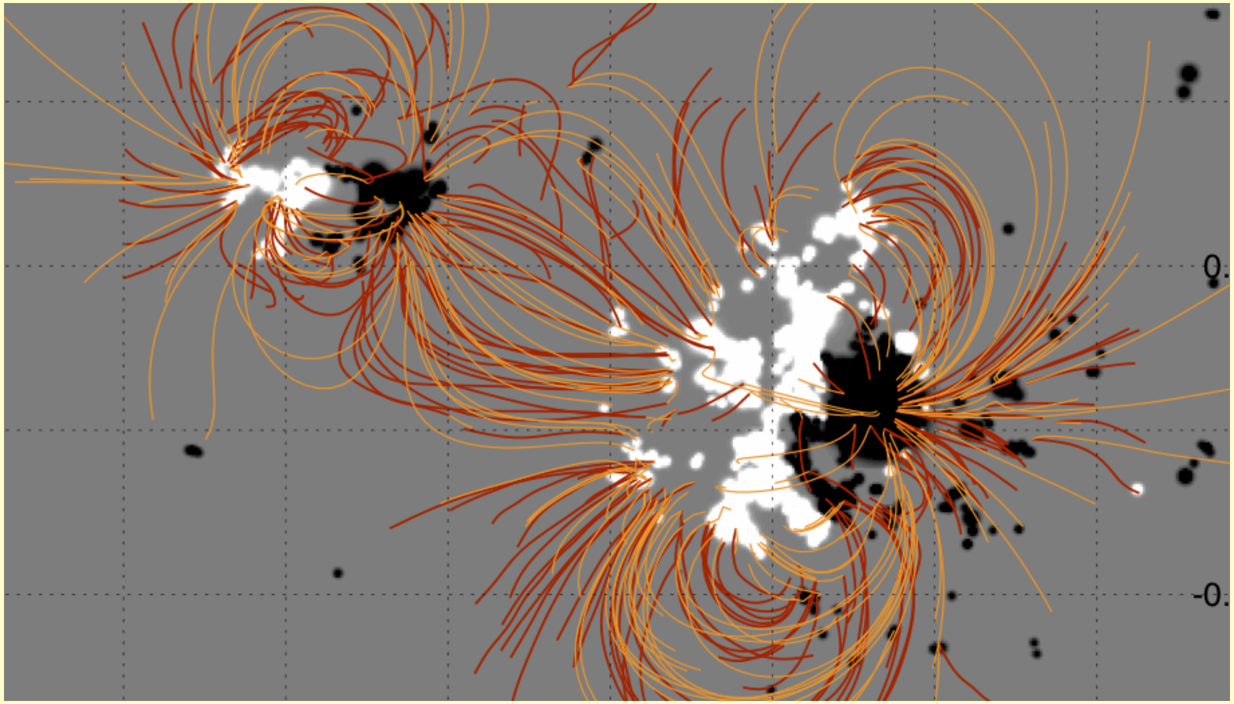

Unipolar potential field
extrapolation and
STEREO loops
A=12.5+15.9 deg

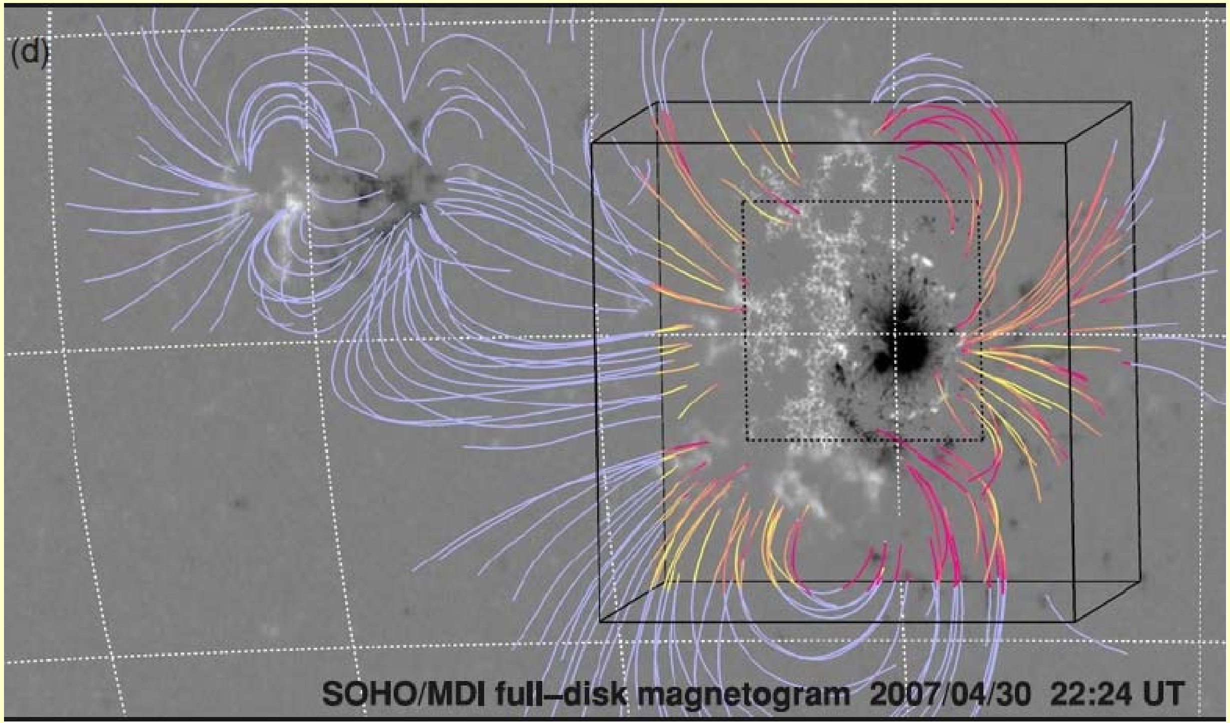

NLFFF extrapolation
(Wheatland code Wh-)
and STEREO loops

Misalignment:
a < 5 deg
a > 45 deg

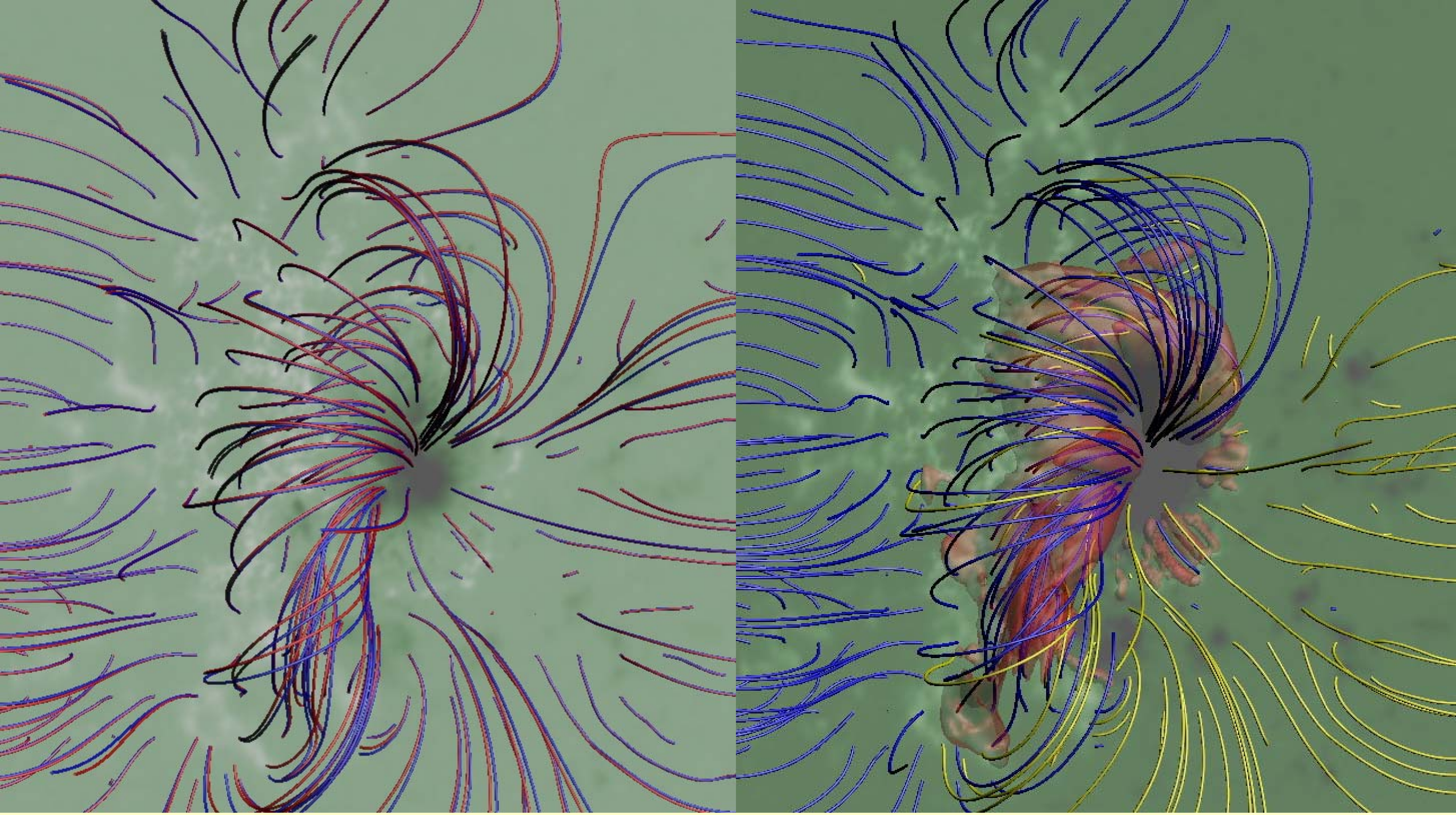

Courtesy of Mike Wheatland and K D Leka

NLFFF (blue and red starting P and N polarity)
Energy E/E0=1.15 (Potential/nonpotential energy)

Two NLFFF solutions, starting from P and N boundaries → significant electric currents.

Case 2: 2007 May 09

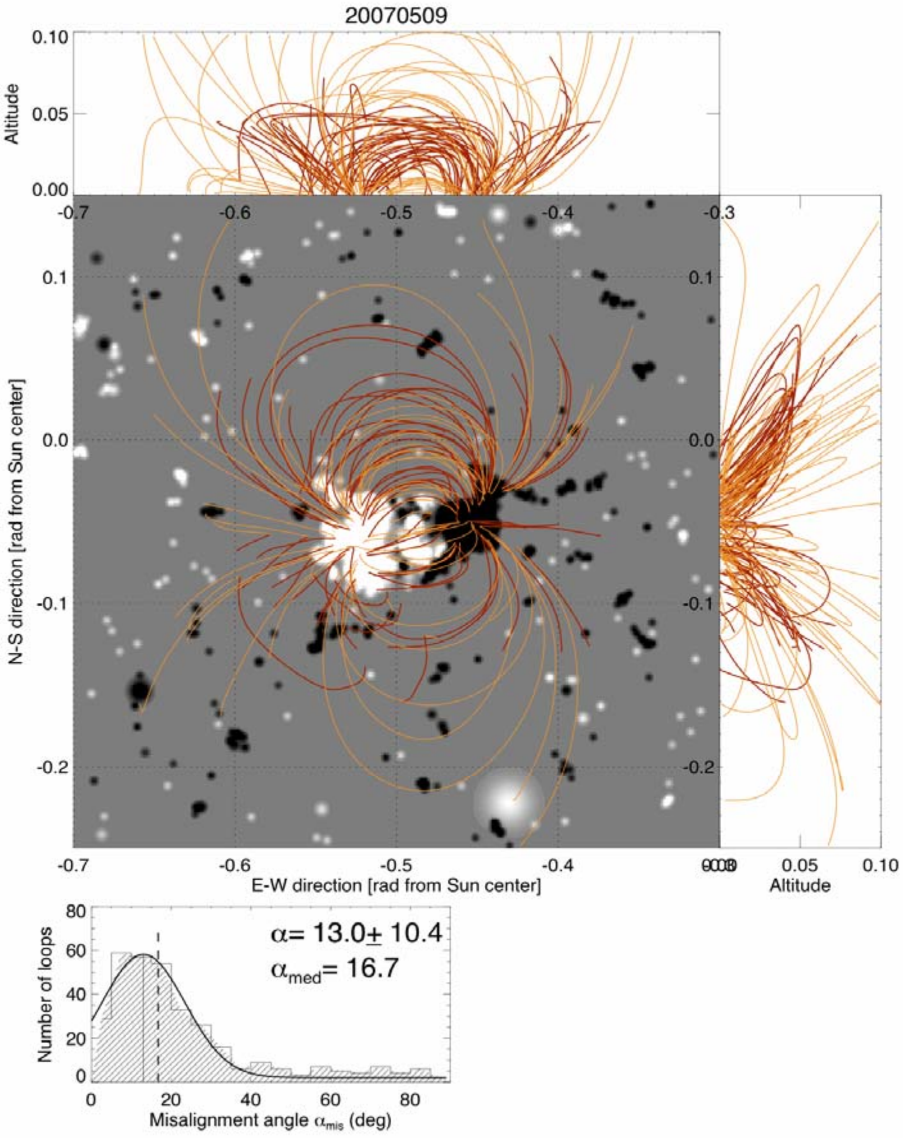

Unipolar potential fiels (n=500)

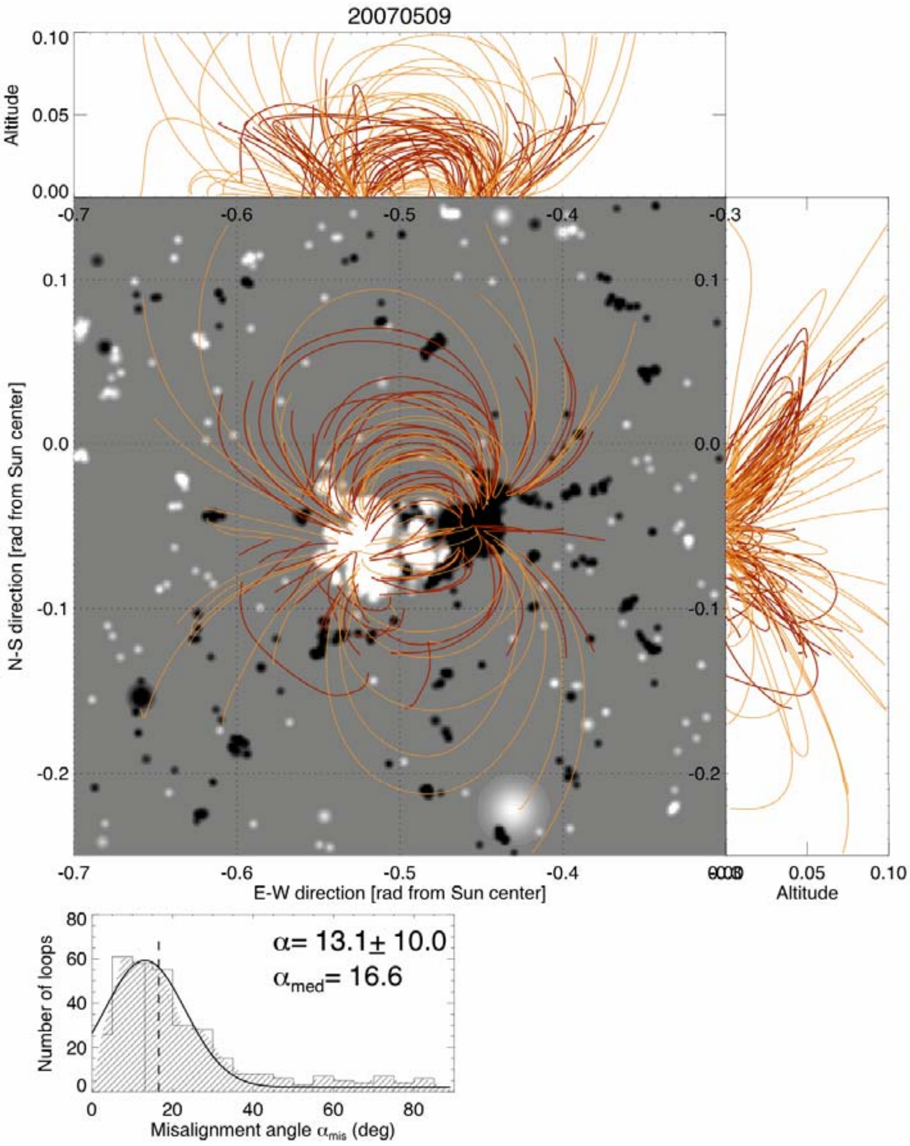

(with forward-fitting of 8 zones with var B)

Case 3: 2007 May 19

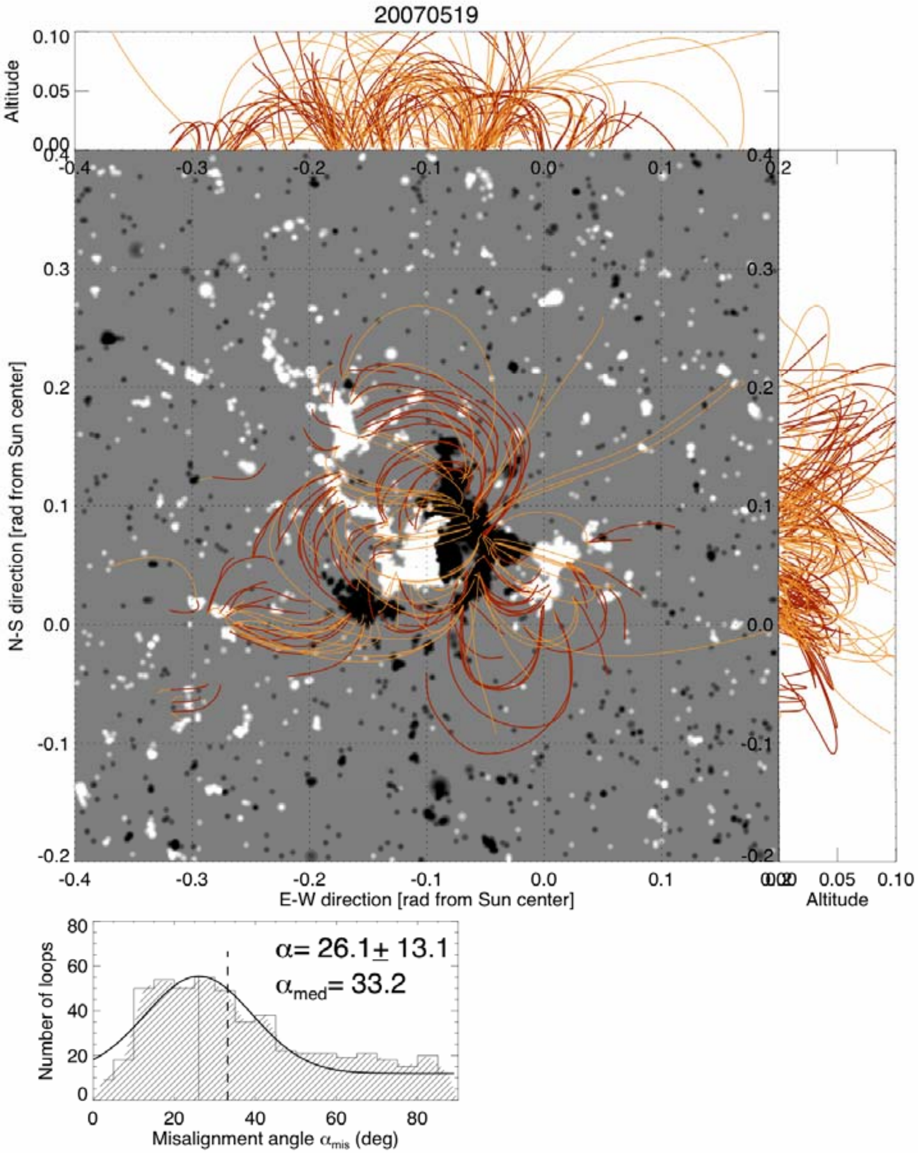

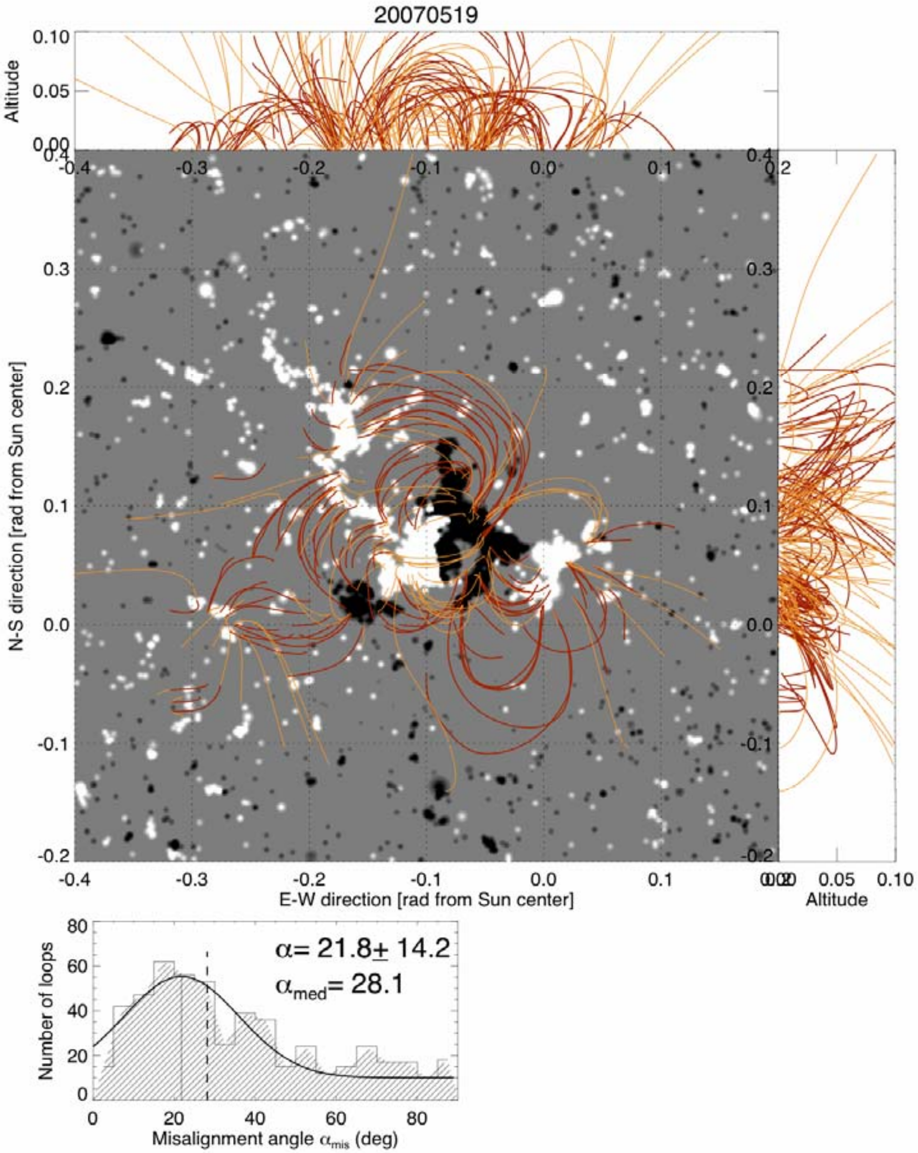

Unipolar potential fiels (n=2000)

(with forward-fitting of 8 zones with var B)

Case 4: 2007 Dec 11

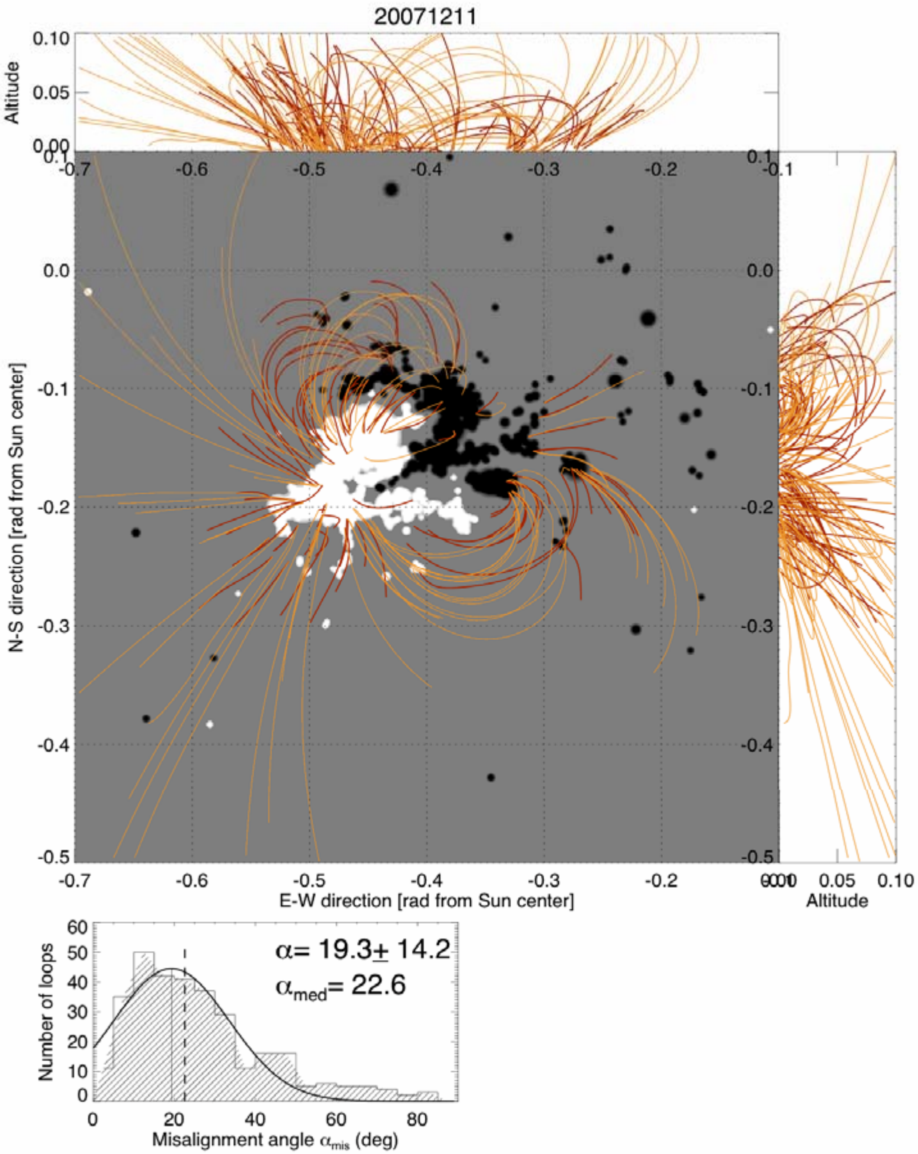

Unipolar potential fiels (n=500)

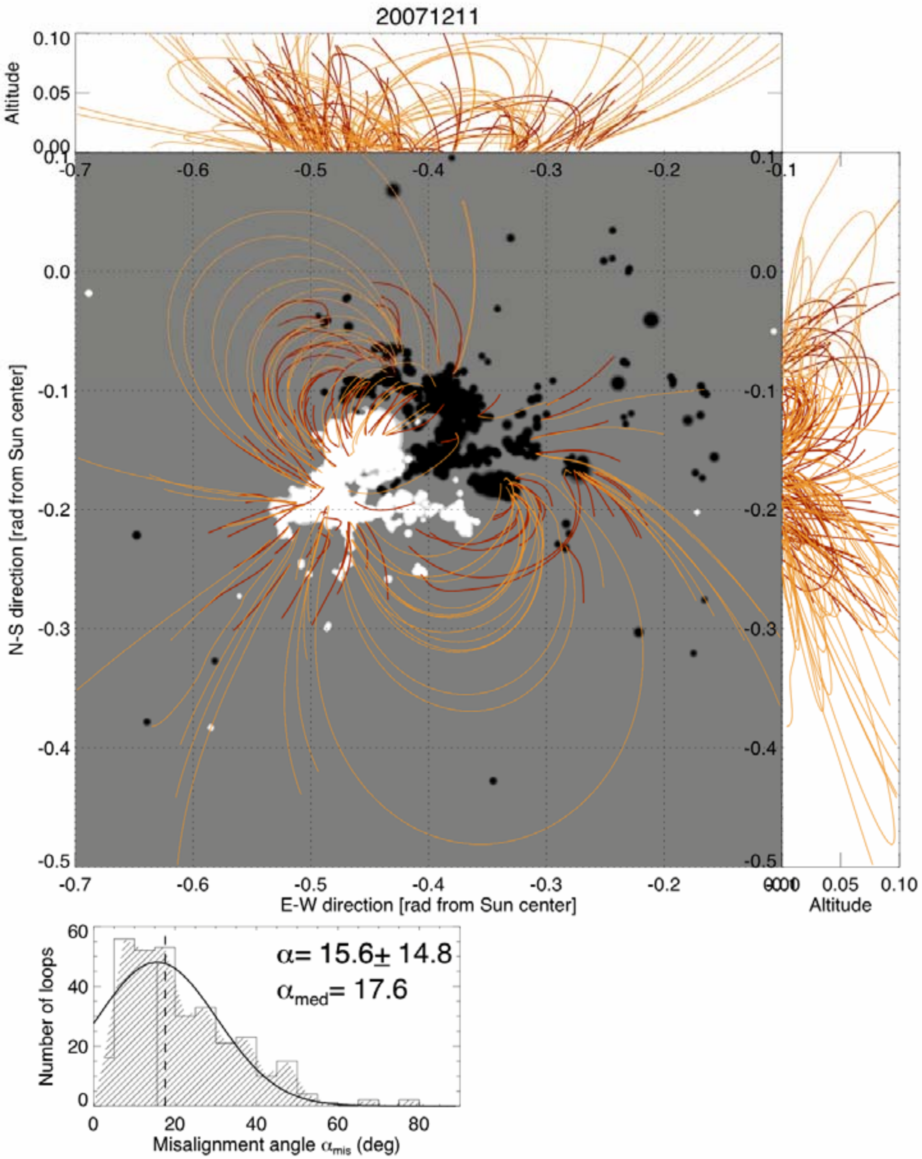

(with forward-fitting of 8 zones with var B)

Comparison of misalignment angles:

	2007 Apr 30	2007 May 09	2007 May 19	2007 Dec 11
PFSS code:				
Sandman et al. 2009:	a = 25 + 8 deg	19 + 6	36 + 13	
DeRosa et al. 2009:	a = 24 deg			
NLFFF codes:				
DeRosa et al. 2009:	a = 24…44 deg			
Unipolar Potential Field:				
n=200	a = 19.3+21.2 deg	13.1+10.0	32.9+16.2	22.2+14.6
n=500	a = 14.5+17.0 deg	13.0+10.4	29.1+13.3	19.3+14.2
n=1000	a = 14.7+13.2 deg	13.9+10.4	26.7+13.2	18.7+12.5
n=2000	a = 15.4+12.2 deg	13.6+10.9	26.1+13.1	19.2+12.5
Unipolar Potential Field Fitting:				
n=200	a = 14.0+12.7 deg	13.6+9.4	23.1+13.0	18.8+9.6
n=500	a = 12.5+15.9 deg	13.1+10.0	20.8+13.1	15.6+14.8
n=1000	a = 14.4+ 9.8 deg	13.4+10.1	21.0+16.0	15.7+13.4
Dipole Potential Field Fitting:				
n=5	a = 16.4+ 7.8 deg	15.4+6.1	24.7+14.4	14.5+6.0
n=10	a = 17.4+ 9.7 deg	12.8+4.3	22.7+10.7	12.4+4.6

SECOND METHOD: Potential field of a dipole

$$\Phi(r,\vartheta,\varphi) = -\left(\frac{z \bullet \cos\vartheta}{r^2}\right), m = \pi a^2 I/c,$$

$$B_r(r,\vartheta) = \nabla\Phi(r,\vartheta) = (B_r, B_\vartheta, B_\varphi) = (2m\cos\vartheta/r^3, m\sin\vartheta/r^3, 0),$$

$$\Delta\Phi(r,\vartheta) = \nabla B(r,\vartheta) = \frac{1}{r^2}\frac{\partial}{\partial r}\left(r^2 \frac{\partial\Phi(r,\vartheta)}{\partial r}\right) = 0.$$

A potential field B(x,y,z) can be represented by a superposition of multiple dipoles:

$$B(x) = \sum_{i=1}^{n} B_i(x) = \sum_{i=1}^{n} \frac{3n(n \bullet m_i) - m_i}{|x|^3},$$

$$r_i = [(x-x_i)^2 + (y-y_i)^2 + (z-z_i)^2]^{1/2},$$

$$n_i = [(x-x_i)/r, (y-y_i)/r, (z-z_i)/r],$$

$$m_i = [m_i \cos\vartheta_i \cos\varphi_i, m_i \cos\vartheta_i \sin\varphi_i, m_i \sin\varphi_i]$$

This parameterized B-field (with 6n parameters B_i,x_i,y_i,z_i, φ_i,ϑ_i) can be forward-fitted to STEREO field lines b=B/|B|.

Unipolar vs. Dipole Potential Field Modeling

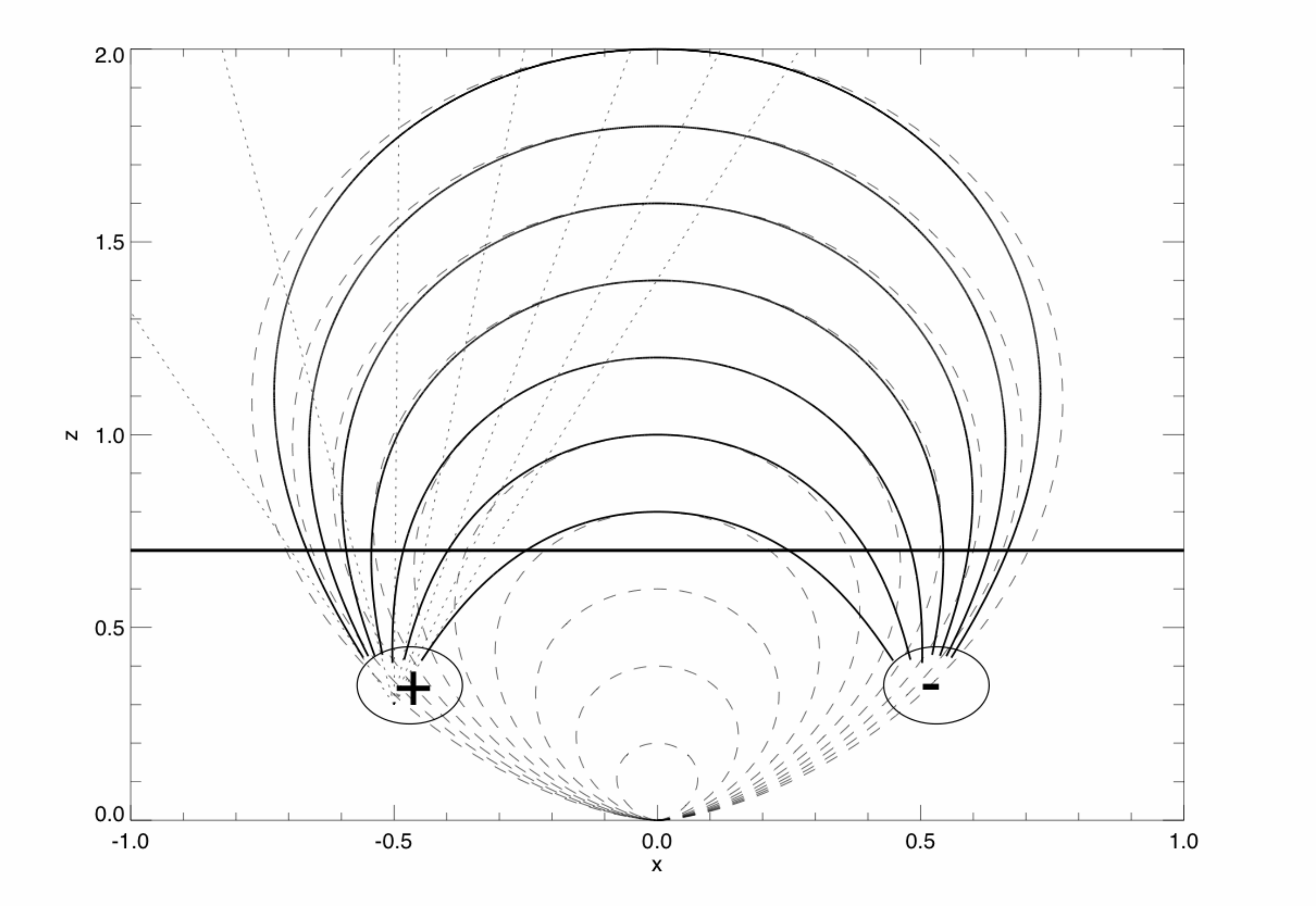

- A dipole is mathematically equivalent to 2 unipolar magnetic charges of opposite sign located at position x=0, z=0.
- Number of parameters: Dipole=6 (m,x,y,z,ϑ,φ) – Unipolar charges=2 x 4 (m,x,y,z)
- Magnetic features with width (w) are burried in depth (z)=(-w)
- Small-scale magnetic features and sharp discontinuities require unipolar components burried in small depths.

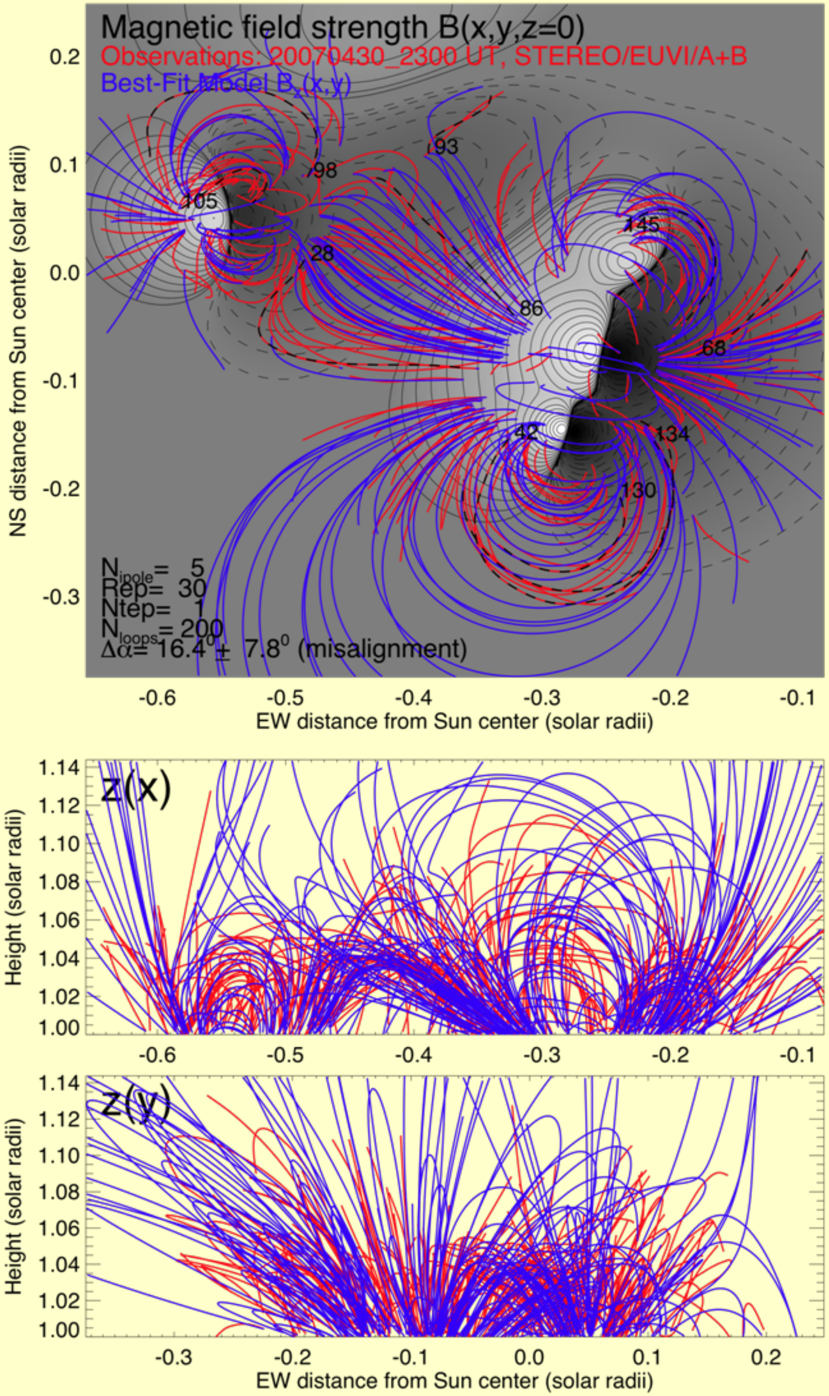

Magnetic field model inferred from STEREO data:

- multiple dipoles (N=6)
- potential field
- divergence free

Forward-fitting of a mutli-dipole field to 3-D STEREO loops yields a smaller misalignment than standard extrapolation of a potential field or Nonlinear force-free field from photospheric magnetograms.

Conclusion: It is not the presence of unaccounted currents or non-potentiality of the coronal magnetic field that causes a large misalignment to observed EUV loops, but rather the inadequacy of photospheric magnetograms (from non-force free regions).

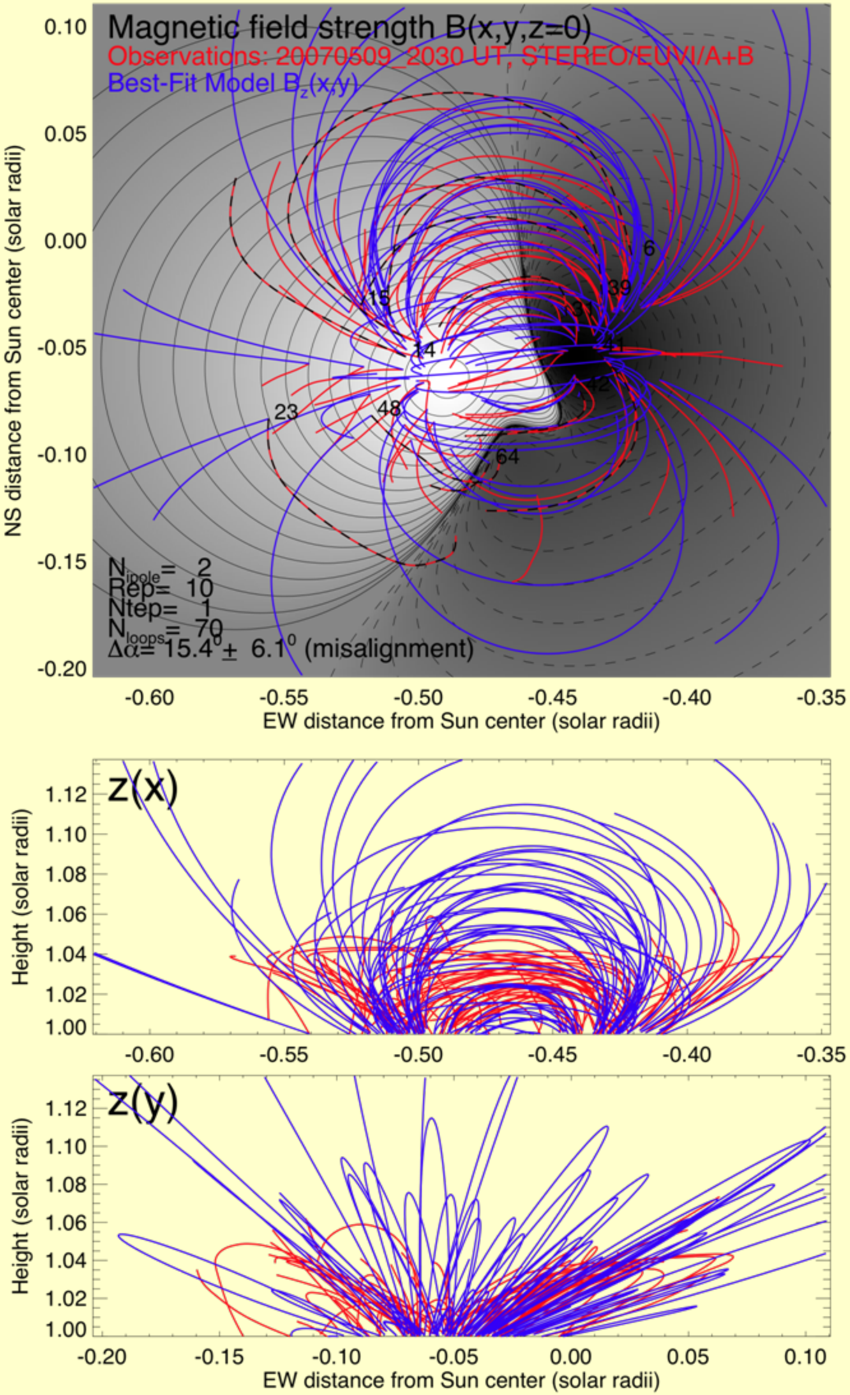
Magnetic field strength B(x,y,z=0)
Observations: 20070509_2030 UT, STEREO/EUVI/A+B
Best-Fit Model $B_z(x,y)$
N_{ipole}= 2
Rep= 10
Ntep= 1
N_{loops}= 70
$\Delta\alpha$= 15.4° ± 6.1° (misalignment)
6
39
15
14
23
48
64
12
NS distance from Sun center (solar radii)
EW distance from Sun center (solar radii)
0.10
0.05
0.00
-0.05
-0.10
-0.15
-0.20
-0.60
-0.55
-0.50
-0.45
-0.40
-0.35
z(x)
Height (solar radii)
1.12
1.10
1.08
1.06
1.04
1.02
1.00
z(y)
-0.20
-0.15
-0.10
-0.05
0.00
0.05
0.10

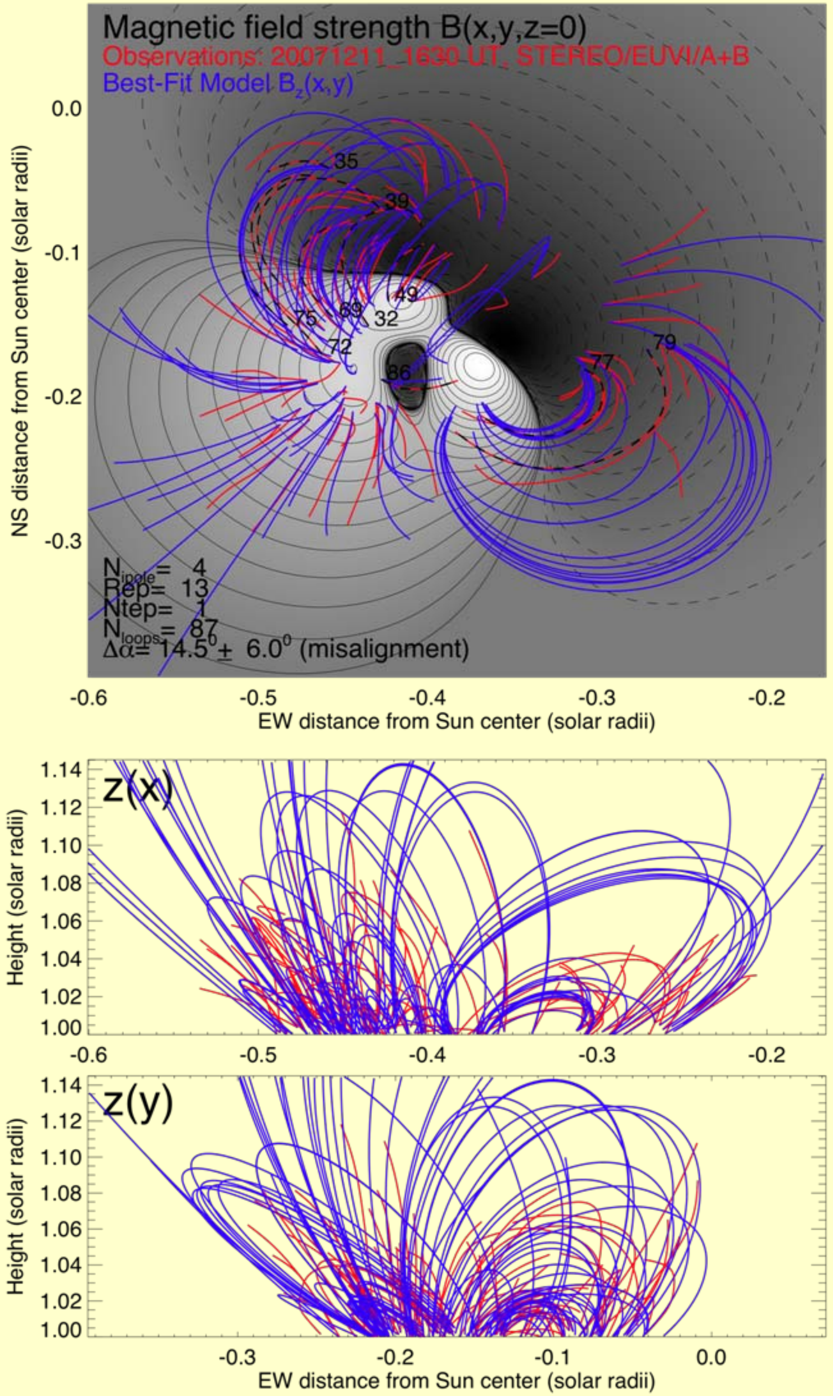
Magnetic field strength B(x,y,z=0)
Observations: 20071211_1630 UT, STEREO/EUVI/A+B
Best-Fit Model $B_z(x,y)$
35
39
49
75
63
32
72
86
77
79
N_{ipole}= 4
Rep= 13
Ntep= 1
N_{loops}= 87
$\Delta\alpha$= 14.5° ± 6.0° (misalignment)
NS distance from Sun center (solar radii)
EW distance from Sun center (solar radii)
0.0
-0.1
-0.2
-0.3
-0.6
-0.5
-0.4
-0.3
-0.2
z(x)
Height (solar radii)
1.14
1.12
1.10
1.08
1.06
1.04
1.02
1.00
z(y)
0.0

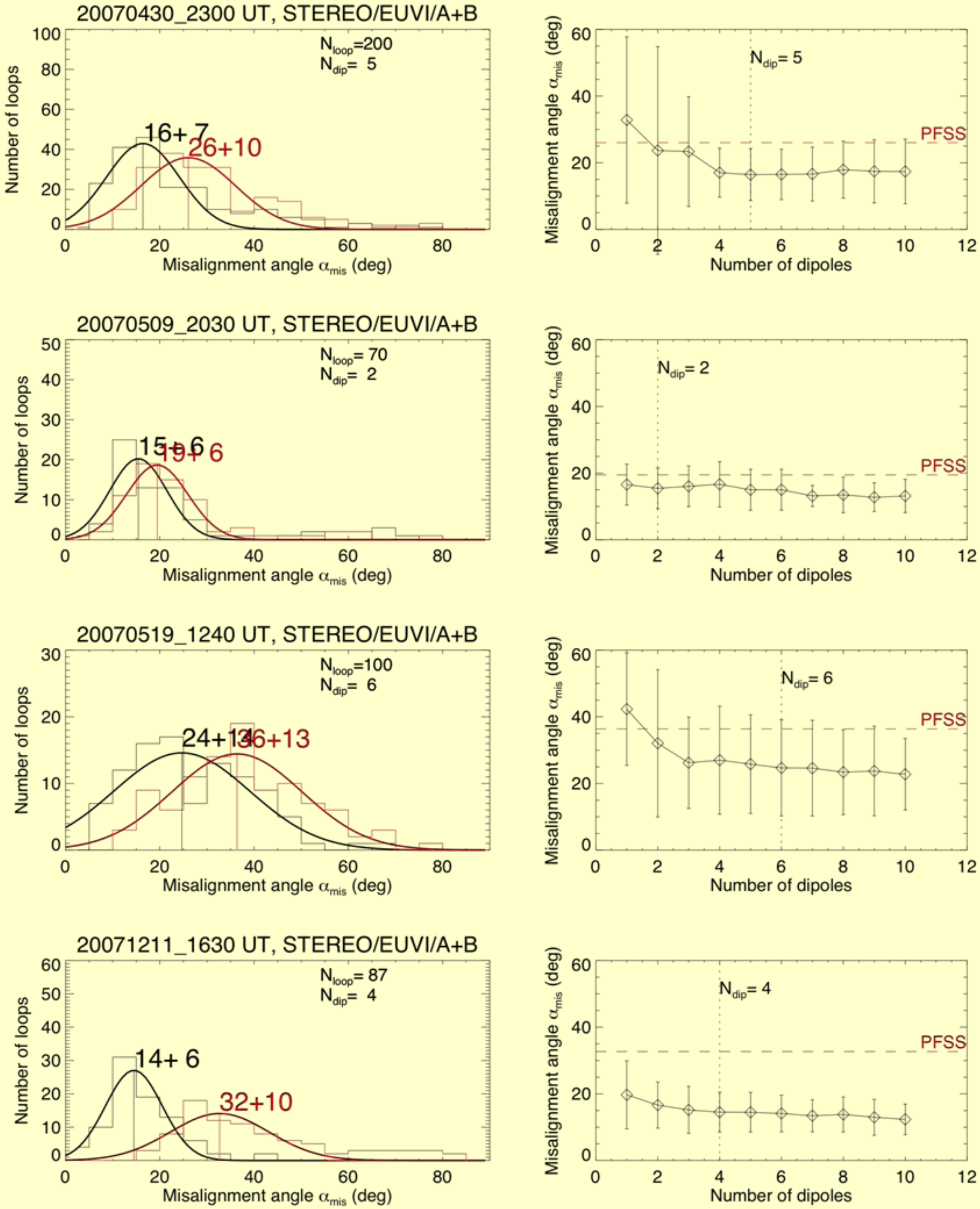
20070430_2300 UT, STEREO/EUVI/A+B
N_{loop}=200
N_{dip}= 5
16+ 7
26+10
Number of loops
Misalignment angle α_{mis} (deg)
N_{dip}= 5
PFSS
Misalignment angle α_{mis} (deg)
Number of dipoles
20070509_2030 UT, STEREO/EUVI/A+B
N_{loop}= 70
N_{dip}= 2
15+ 6
19+ 6
Number of loops
Misalignment angle α_{mis} (deg)
N_{dip}= 2
PFSS
Misalignment angle α_{mis} (deg)
Number of dipoles
20070519_1240 UT, STEREO/EUVI/A+B
N_{loop}=100
N_{dip}= 6
24+14
36+13
Number of loops
Misalignment angle α_{mis} (deg)
N_{dip}= 6
PFSS
Misalignment angle α_{mis} (deg)
Number of dipoles
20071211_1630 UT, STEREO/EUVI/A+B
N_{loop}= 87
N_{dip}= 4
14+ 6
32+10
Number of loops
Misalignment angle α_{mis} (deg)
N_{dip}= 4
PFSS
Misalignment angle α_{mis} (deg)
Number of dipoles

Conclusions

1) The observations of stereoscopically triangulated 3D geometries of coronal loops in ARs exhibit a discrepancy to theoretical magnetic field models based on extrapolations of photospheric magnetograms, with a typical misalignment angle of a=19-36 deg (PSFF) and a=24-44 deg (NLFFF).

2)Hypothesis: The photospheric field is not force-free.

3)Magnetic potential field extrapolations using a parameterization with unipolar magnetic charges and dipoles yield a better agreement of a=14-26 deg, which seems to indicate that a higher spatial resolution (than PSFF) in potential field codes improves consistency with STEREO.

4)A bootstrapping method with forward-fitting of free parameters in (unipolar and dipole) potential field models improves agreement with STEREO further, a=12-23 deg.

5)The remaining misalignment of a=12-23 deg could be due to:
   (a) coalignment inaccuracy (MDI+EUVI) and insufficient spatial resolution
   (b) neglect of projection effects, longitudinal field, and curvature in bootstrap model
   (c) stereoscopic triangulation errors (check consistency of adjacent loops !)
   (d) non-potentiality of magnetic field (requires NLFFF modeling)

http://www.lmsal.com/~aschwand/ppt/2010_STEREO_Dublin.ppt